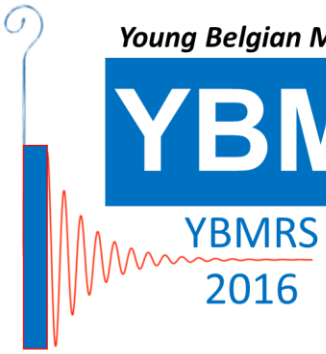

Young Belgian Magnetic Resonance Scientists

YBMRS 2016

15th edition

5th and 6th December 2016

PROGRAM AND ABSTRACT BOOK

YBMRS 2016

Dear YBMRS Participant,

Welcome to the 15th edition of the Young Belgian Magnetic Resonance Scientist symposium series!

We thank you for joining us and hope you will enjoy the conference, as well as your stay here in the heart of the most beautiful Belgian forest. The organizers have strived to present an attractive program, including two educational sessions, two invited lectures and a selection of short oral communications on a wide variety of topics. As always, the goal has been to promote the work of young scientists working in any field related to magnetic resonance, and to create opportunities for interesting discussions and contacts.

General practical information

All scientific activities are organized around the "Pierre le Grand" conference room, which can be found to the right from the main in the lobby at the level -1. All participating sponsors are located in the meeting area of the Sol Cress, where coffee breaks will be served during the poster sessions and in between the morning sessions. A wardrobe is available, however we urge you not to leave any valuables as we cannot guarantee it will be guarded at all times. Should you have any question during your stay, please address yourself to the conference desk located in the meeting area.

During sessions

- Please switch off your mobile phone or put it in silent mode.
- Do not take pictures of slides or posters, but rather approach the author during the meeting and request a reprint or additional information.
- Have the courtesy not to use your laptop in the conference room during talks, but rather use the main lobby, foyer or bar.

Poster sessions

All posters are to be set up in the "Wellington" and "Sources de la Reine" rooms. The posters panels are numbered. Your poster number is available from the abstract book or on the list provided in the poster room. Participants presenting a poster are kindly requested to set up their poster no later than the lunch break on Monday, and to remove them after the coffee break on Tuesday afternoon. Transparent adhesive tape is available in the poster room to fix your poster to the panels. Please do not use staples or pushpins in any circumstances.

Rooms

If you have not done so, please register for your room at the main desk in the lobby of the Sol Cress.

Check out time: Please note that all rooms should be vacated no later than 10:00 a.m. on Tuesday morning.

A closed luggage room, next to the poster room, will be available on Tuesday for safekeeping of your luggage. Should you have any question or request concerning your accommodation, please contact the Sol Cress staff.

Breakfast, lunch and dinner

Breakfast and lunch will be served in the Restaurant. Please follow the indications from the main lobby. Breakfast is served from 07:30 until 09:00 on Monday and Tuesday morning. Lunch starts immediately after the morning session and consists of a buffet with beverages on Monday and of a hot meal on Tuesday.

The main conference dinner will start at 20:00 on Monday evening, with a choice between a vegetarian or a non-vegetarian menu, as indicated during your registration.

If you have any additional dietary requirements, please contact the Sol Cress staff.

Internet access

Free wireless internet access is available in the entire domain.

YBMRS party

A party will be organized after dinner on Monday evening, starting around 10 p.m. and featuring the House DJ.

At the request of the Sol Cress, and as a courtesy to the other guests, please note that the party is set to close at 01:00.

Please note that the bar remains available to provide more tranquil surrounding. If you have further questions, please contact the conference desk in the foyer.

Yours sincerely,

The Organizing Committee

- C. Aprile, UNamur
- L. Fusaro, UNamur
- B. Gallez, UCL
- B. Jordan, UCL
- S. Acciardo, UCL
- L. A. Bivona, UNamur
- E. Carbonell, UNamur
- A. Comes, UNamur
- P. Danhier, UCL
- L. Mignion, UCL
- A. Vivian, UNamur

The Scientific Committee

- C. Aprile, UNamur
- K. Bartik, ULB
- G. Bruylants, ULB
- C. Damblon, ULg
- P. de Tullio, ULg
- L. Fusaro, UNamur
- B. Gallez, UCL
- Y. Gossuin, UMONS
- U. Himmelreich, KUL
- B. Jordan, UCL
- S. Laurent, UMONS
- M. Luhmer, ULB
- J.C. Martins, UGent
- L. Vander Elst, UMONS
- S. Van Doorslaer, UAntwerpen
- A. Volkov, VUB

The organizing committee gratefully acknowledges the following institutions, societies and companies for their kind support

Platinum Sponsors

Golden Sponsors

Silver Sponsors

Symposium Program

Monday, 5th December

9:30 **Registration, wake-up coffee, poster setup**

10:50 **Welcome:** *Chair C. Aprile*

Educational Session

11:00 Michel Luhmer (ULB): **Structure elucidation of organic compounds by solution-state NMR spectroscopy: basics, strategy and case studies**

12:00 Christian Damblon (ULg): **How can NMR contribute to protein science?**

13:00 **Lunch**

Plenary Session 1: *Chair D. Sinnaeve*

14:30 Loic Capette (UMONS): **Dendrimers like platforms for molecular imaging: characterization of successive generations of paramagnetic dendrimers. Evaluation and perspectives**

14:50 Glenn Grawels (ULB): **Physico-Chemical Characterisation of Chloride Transmembrane Transport using Calix[6]arene-based Receptors**

15:10 Niels Geudens (UGent): **Membrane Interactions of Cyclic Lipodepsipeptides**

15:30 **Flash presentation 1** (1:30 min each) of posters with odd number

16:00 **Poster session 1** (odd number) **- Coffee break**

Plenary Session 2: *Chair B. Jordan*

17:30 Invited Speaker - Kevin Brindle (University of Cambridge): **Molecular imaging of metabolism using hyperpolarized substrates**

18:30 PI Meeting

19:00 **Reception and Free Time for Discussion**

20:00 **Dinner and YBMRS party**

Tuesday, 6th December

Plenary Session 3: *Chair Adriaensens*

9:00 Marie-Aline Neveu (UCL): **Multi-modality imaging to assess metabolic shift in tumors**

9:20 Silvanose Biju (KU Leuven): **Lanthanide (Dy^{3+}, Ho^{3+}) doped upconversion (NIR-NIR) nano-architecture as multimodel contrast agents for next generation MRI and Optical imaging**

9:40 Emilio Brunetti (ULB): **Mechanism of guest exchange in the cavity of a biomimetic calix[6]arene based receptor: input of 1D EXSY NMR**

10:00 **Flash presentation** (1:30 min each) of posters with even number

10:30 **Poster session** (even number) **- Coffee break**

Plenary Session 4: *Chair A. Volkov*

12:00 Ulric Le Paige (Leiden Universiteit): **Magnetic inequivalence in an isotope-labelled trimethyl amine: complicated yet simple spectrum or simple yet complicated spectrum?**

12:20 Marius Wanko (ULg): **Rapid protein structure determination using experimental NMR data**

12:40 Kevin Nys (UAntwerpen): **Characterizing haemoglobin of the European honeybee and the malaria mosquito using optical and EPR spectroscopy**

13:00 **Bruker oral communication**

13:05 **Lunch**

Plenary Session 5: *Chair L. Fusaro*

14:30 Invited Speaker – Laurent Delevoye (Université de Lille ST): **Advanced solid-state NMR as a key tool for the deeper understanding of heterogeneous catalysts**

15:30 Pierre Danhier (UCL): **Fate of intracellular iron oxides in magnetic cell tracking studies**

15:50 Esther Carbonell (UNamur): **Self-Assembly of Silsesquioxane-based structures for the Design of 3D Polymeric Network**

16:10 Krizstina Fehér (UGent): **Effects of conformational flexibility on protein function as probed by NMR spectroscopy and Molecular Dynamics simulations**

16:30 **Coffee Break & Poster Removal**

17:00 **Awards & closing** *Chair B. Gallez*

LIST OF POSTERS

P1 S. Acciardo, L. Mignion, B. Gallez and B. F. Jordan.

Imaging markers of response to combined BRAF - MEK inhibition in melanoma

P2 T.-T. Cao-Pham, N. Joudiou, B. Gallez, B.F. Jordan

Combined endogenous MR biomarkers to predict tumour basal oxygenation and response to hyperoxic challenge

P3 S. Chilla, G. Hallot, S. Lacroix, G. Doumont, S. Boutry, L. Vander Elst, S. Goldman, R.N. Muller, S. Laurent.

Development of a bimodal contrast agent for MRI and PET scan

P4 W. Denis, E. Amadio, G. Grauwels, K. Bartik, G. Licini

Towards Lignin Valorisation: NMR Characterisation of Oxidative Cleavage Reactions using Micellar Vanadium-based Catalytic Systems

P5 C. Desmet, G. Vandermeulen, V. Préat, Ph. Levêque, B. Gallez

Oxygenation (measured by EPR) is a predictive marker of wound healing in diabetic mice

P6 J. Diricq, D. Stanicki, L. Vander Elst, S. Laurent

From SiO precursor to bimodal probe : An innovative way to target inflammation?

P7 L. Fusaro, V. Ndoyom, T. Roisnel, V. Dorcet, B. Boitrel and S. Le Gac

Mono- and bimetallic porphyrin-based complexes: what we can learn from heteronuclear NMR?

P8 K. Govaerts, J. Sternisa, J.R. Rangarajan, F. Van Leuven, U. Himmelreich

The effect of a high-fat, high-sugar Western-type diet on brain volumetrics of APP-PS1 transgenic animals

P9 Z. Hafideddine, S. Dewilde, S. V. Doorslaer

Using globins in biosensors

P10 A. Hannecart, D. Stanicki, L. Vander Elst, L. Mespouille, R. N. Muller, S. Laurent

Clustering of iron oxide nanoparticles into poly(ethylene oxide)-block-poly(ε-caprolactone) nanoassemblies as ultrasensitive MRI probes

P11 E. Hequet , C. Henoumont , R. Muller, L. Vander Elst, S. Laurent

Synthesis and characterisation of fluorinated paramagnetic contrast agents for their use in ^{19}F MRI

P12 J. Kay, T. Banelli, M. Vuano, D. C. Thorn, S. Preumont, F. Fogolari, C. Damblon, A. Corazza and M. Dumoulin

Investigation of the effects due to the insertion of a polyQ tract increasingly long on the structure and dynamic of BlaP using NMR spectroscopy

P13 B. Kovács, É. Dorkó, B. Kótai, A. Domján, T. Soós

Is it possible, that a Lewis acid has revolving acid strengths?

P14 T. K. N. Luong, P. Shestakova and T. N. Parac-Vogt

Kinetic studies of phosphoester hydrolysis promoted by a dimeric tetrazirconium(IV) Wells-Dawson polyoxometalate by NMR spectroscopy

P15 H. G. T. Ly, G. Fu, D. De Vos, and T. N. Parac-Vogt

Application of MOFs as Heterogeneous Catalysts for Hydrolysis of Peptides

P16 R. Michez, J. Vander Steen, Th. Doneux, C. Buess-Herman and M. Luhmer

Influence of the Electrode Material on the Electrochemical Stability of an Imidazolium-based Ionic Liquids by NMR Spectroscopy

P17 S. Montante, R. N. Muller, L. Vander Elst, S. Laurent

Design of An Effective Bimodal Diamond-based Nanoprobe for Biomedical Purposes

P18 E. Ottoy, G. J. Hofman, J. C. Martins, B. J. Linclau and D. Sinnaeve

Analysis of the five-membered ring pucker of β- and γ-fluorinated prolines by means of NMR spectroscopy and pseudorotation theory

P19 S.A. Pötgens, N.M. Delzenne and L.B. Bindels

Using NMR metabolomics to unravel the pathways underlying the host-microbiota crosstalk in cancer cachexia

P20 M. Retout, H. Valkenier, and G. Bruylants

Simple and direct method to quantify PEG molecules grafted on gold nanoparticles using ^{1}H NMR spectroscopy

P21 S. Scheinok, P. Levêque, P. Sonveaux and B. Gallez.

Development of a sensitive and specific assay to measure mitochondrial superoxide in tumor cells

P22 F. Souard, V. Piras, R. D'Orazio, L. Stefanosaka, F. Dufrasne, P. Stoffelen, C. Stévigny and M. Luhmer

Palladium-based chemosensors for the characterization of raw plant extracts by ^{19}F NMR spectroscopy

P23 M. Tassi, G. Reekmans, J. D'Haen, R. Carleer, P. Adriaensens

^{31}P solid state NMR for the quantitative characterization of TiO_2 nanopowders modified with phosphonic acids

P24 T. Vangijzegem, D. Stanicki, S. Boutry, R.N. Muller, L. Vander Elst, S. Laurent

Synthesis and characterization of a nanoparticulate T_1 contrast agent for magnetic resonance imaging

P25 M. Van Landeghem, E. Goovaerts, S. Van Doorslaer

EPR study of lead-free $MA_2CuCl_xBr_{4-x}$ hybrid perovskites for photovoltaics

P26 A. Vivian, L. Fusaro, D. P. Debecker and C. Aprile

Porous Sn-silicate catalysts prepared via aerosol-assisted sol-gel process

INVITED LECTURES

Imaging tumour metabolism with hyperpolarized ^{13}C-labeled cell substrates

K. M. Brindle

Department of Biochemistry, University of Cambridge, Tennis Court Road, Cambridge CB2 1GA, UK and Cancer Research UK Cambridge Institute, Li Ka Shing Centre, University of Cambridge, Robinson Way, Cambridge, CB2 0RE, UK
email: kmb1001@cam.ac.uk

Molecular imaging could play an important role in predicting and detecting tumor responses to treatment and thus in guiding treatment in individual patients [1]. Nuclear spin hyperpolarization can increase sensitivity in the magnetic resonance experiment by >10,000x. This has allowed imaging of injected hyperpolarized ^{13}C labelled cell substrates *in vivo* and, more importantly, their metabolic conversion into other metabolites. We have been using this metabolic imaging technique both to detect treatment response and to investigate the tumor microenvironment. A recent perspective on this field of research is given in [2]. Exchange of hyperpolarized ^{13}C label between lactate and pyruvate and net flux of label between glucose and lactate have been shown to decrease post-treatment and hyperpolarized [1,4-^{13}C]fumarate has been shown to detect subsequent cell necrosis. Tumor pH can be imaged using hyperpolarized $H^{13}CO_3^-$ and redox state can be determined by monitoring the oxidation and reduction of [1-^{13}C]ascorbate and [1-^{13}C]dehydroascorbate respectively. In this talk I will discuss more recent work in which we have used hyperpolarized [1-^{13}C]pyruvate to investigate metabolism in PDX models of glioblastoma. These measurements have shown significant heterogeneity between tumours derived from different patients, which we believe is related to underlying oncogenic mutations. I will also show how hyperpolarized [1-^{13}C]pyruvate can be used to follow the progression of pancreatic precursor lesions, in a genetically engineered mouse model of the disease, which potentially could be used clinically to guide earlier intervention [3]. Finally I will discuss how we have used hyperpolarized [U-^{2}H, U-^{13}C]glucose [4] to investigate flux in the pentose phosphate pathway (PPP) and the relationship between PPP flux and the rate of reduction of hyperpolarized [1-^{13}C]dehydroascorbate.

Metabolic imaging with hyperpolarized ^{13}C-labelled cell substrates has recently translated to the clinic with a study in prostate cancer [5] and we have conducted our first clinical study in Cambridge using this technique earlier this year.

1. Brindle, K. *Nature Rev Cancer* 2008, **8**, 94-107.
2. Brindle, K.M. *J. Amer. Chem. Soc.* 2015, **137**, 6418-6427.
3. Serrao, E.M.*, et al. Gut* 2016, **65**, 465–475.
4. Rodrigues, T.B.*, et al. Nat Med* 2014, **20**, 93-97.
5. Nelson, S.J.*, et al. Science Translational Medicine* 2013, **5**, 198ra108.

Advanced Solid-State NMR as a Key Tool for the Deeper Understanding of Heterogeneous Catalysts.

D. Grekov[1], Y. Bouhoute[2], N. Merle[2], I. Del Rosal[3], L. Maron[3], M. Taoufik[2], R. Gauvin[1] and L. Delevoye[1]

[1] UCCS, CNRS UMR 8181, Université de Lille ST, F-59655 Villeneuve d'Ascq.
[2] C2P2, CNRS UMR 5265, ESCPE Lyon, F-69616 Villeurbanne.
[3] LPCNO, CNRS UMR 5215, Université de Toulouse, INSA, UPS, F-31077 Toulouse.

The immobilization of organometallics onto inorganic carriers is an attractive option for the synthesis of heterogeneous catalysts that would feature (ideally) well-defined surface sites. This requires understanding of organometallic-surface reactivity that is specific for a given support. In some instance, several types of grafted species can be obtained, depending on surface reaction sites or on molecular precursor's reactivity. This impacts on catalysis as both metal-support interactions and metal coordination sphere have a strong influence on these systems' performances.

In this context, solid-state NMR is a key technique, as it provides information at the molecular level, with fast technical and methodological developments. Many nuclei from the periodic table are NMR sensitive, with more than 75% being quadrupolar nuclei (spin I>1/2). Thanks to high resolution (MQ MAS), homonuclear (DQ MAS) and heteronuclear (HMQC) techniques, it is nowadays possible to extract precise structural information on surface-grafted species, even for quadrupolar nuclei of low natural abundance (i.e. oxygen-17).

In this contribution, we first present some of the latest methodological developments to improve the sensitivity and resolution in the NMR study of quadrupolar nuclei. This involves the use of 2D HMQC-type pulse sequences, which provide information about either proximity and connectivity between hetero-atoms.

Then, thanks to advanced NMR methods, along with DFT calculations of NMR parameters, we show how it is possible to unveil some key structural elements on selected examples in the field of supported catalysis:

- Surface-selective ^{17}O labelling of silica provides information on the interactions between grafted organometallic fragments and the support.[1]
- Structural assignment of silica-supported tungsten oxo (organometallic) species for alkene metathesis can be achieved thanks to ^{17}O NMR.[2]
- Selective and efficient ^{1}H-^{27}Al heteronuclear correlations provide a fresh view on the alumina hydroxyl groups network and on its surface chemistry.[3]

1. Merle, N., Trébosc, J., Baudouin, A., Del Rosal, I., Maron, L., Szeto, K., Genelot, M., Mortreux, A., Taoufik, M., Delevoye L., and Gauvin, R.M. *J. Am. Chem. Soc.* 2012, **134**, 9263.
2. Merle, N., Girard, G., Popoff, N., De Mallmann, A., Trébosc, J., Berrier, E., Paul, J.-F., Del Rosal, I., Maron, L., Gauvin, R. M., Delevoye, L. and Taoufik, M. *Inorg. Chem.* 2013, **52**, 10119.
3. Taoufik, M., Szeto, K. C., Merle, N., Del Rosal, I., Maron, L., Trébosc, J., Tricot, G., Gauvin, R. M., and Delevoye, L. *Chem. Eur. J.* 2014, **20**, 4038.

EDUCATIONAL LECTURES

Structure elucidation of organic compounds by solution-state NMR spectroscopy: basics, strategy and case studies.

M. Luhmer

Laboratoire de Résonance Magnétique Nucléaire Haute Résolution (RMN-HR)
Université libre de Bruxelles – ULB CP 160/08

michel.luhmer@ulb.ac.be

This tutorial focusses on the structure characterization of small- to medium-sized diamagnetic organic compounds by ^{1}H and ^{13}C solution-state NMR spectroscopy.

It briefly reviews the most important underlying concepts, discusses the interpretation of common one- and two-dimensional spectra, and provides guidelines for a systematic approach, which will be illustrated by the elucidation of the structure of a compound with formula $C_{10}H_{20}O$.

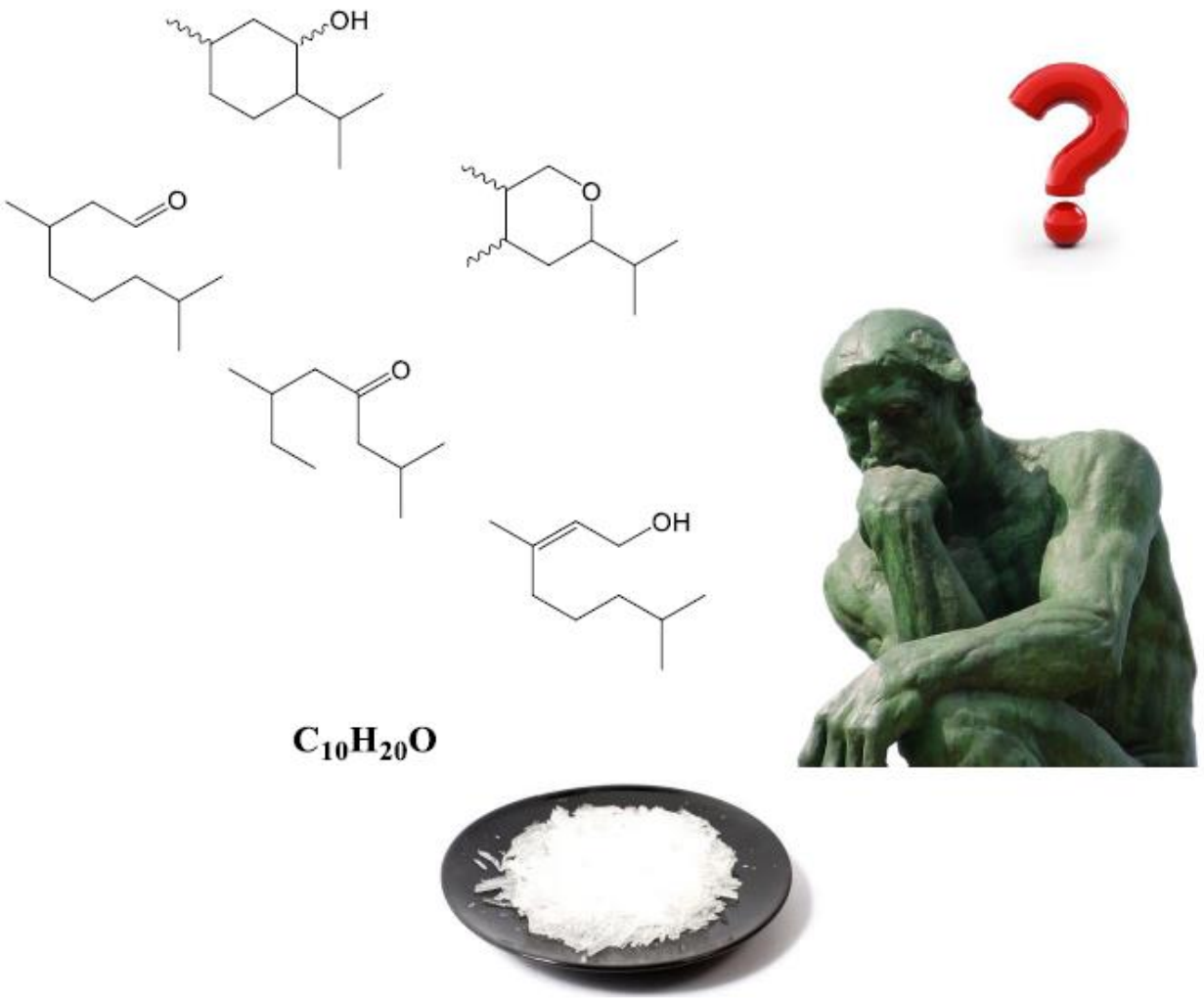

How can NMR contribute to protein science?

C. Damblon

Department of Chemistry, University of Liège

NMR is widely used to characterise molecules isolated from nature or synthesised by organic chemistry. Chemical structures, 3D structures, dynamics can be determined thanks to NMR. But signal overlap makes resolution a serious issue and becomes a limitation when the molecular weight is too large. With proteins of several thousands Dalton, NMR seems to be inappropriate to produce detail analyses. However from the very beginning of NMR as an analytical technique, some brave spectroscopists collaborating with biologists have used NMR to study complex and large biological macromolecules.

The fascination of some spectroscopists for biological macromolecules has led to remarkable developments towards protein science and eventually to a Nobel Prize in 2002 for the demonstration of the feasibility of protein 3D structure determination with only NMR spectroscopy. If the first structure obtained in 1985 was for a small 6000 Da protein, tremendous progresses have been made since and at the present time 3D structures have been determined for proteins of 50000 Da.

The purpose of this lecture is to review the NMR applications that contribute to the analysis of protein structures, interactions and dynamics.

YOUNG RESEARCHER ORAL COMMUNICATIONS

Dendrimers like platforms for molecular imaging: characterization of successive generations of paramagnetic dendrimers. Evaluation and perspectives

L. Capette[1], S. Laurent[1,2], S. Boutry[2], L. Granato[1], R. N. Muller[1,2] and L. Vander Elst[1,2]

[1] NMR and Molecular Imaging Laboratory, University of Mons.
[2] Center for Microscopy and Molecular Imaging, Charleroi, Belgium.

Dendrimers are a class of particular polymers with a large number of functions and a rigid quasi-spherical structure. Their properties make them ideal for a wide range of biomedical applications.

The aim of this work is therefore the development of a macromolecular contrast agent with several paramagnetic centers with a reduced mobility, able to be transported by neurons. Indeed, previous studies showed that the reduction of the mobility of a Gd-complex increases its efficiency in the magnetic fields of medical imaging.

In this objective, we considered the multistep synthesis of a selective paramagnetic dendrimeric contrast agent. Up to now, the three generations of paramagnetic dendrimers have been successfully synthesized by optimizing different synthesis parameters such as the solvents, temperature, reaction time and reagents. Finally, all generations were characterized by mass spectrometry and by nuclear magnetic resonance (NMR) spectroscopy.

Their comparative study with the commercial Dotarem® shows that at 60 MHz (the medical magnetic field) and 37°C, the relaxivity for the generation zero is 6.13 $s^{-1}mM^{-1}$ by Gd ion (**12.25 $s^{-1}mM^{-1}$** per molecule). For the generation one, it is 9.71 $s^{-1}mM^{-1}$ by Gd ion (**38.84 $s^{-1}mM^{-1}$** per molecule) and for the generation two, it is 12.13 $s^{-1}mM^{-1}$ by Gd ion (**97.04 $s^{-1}mM^{-1}$** per molecule). These results represent a substantial gain in term of relaxivity, as compared with the Dotarem® alone (3.06 $s^{-1}mM^{-1}$).

We are currently investigating the grafting of the biocytin on the second generation of dendrimers in order to obtain a MRI contrast agent able to undergo uptake and transport by neurons.

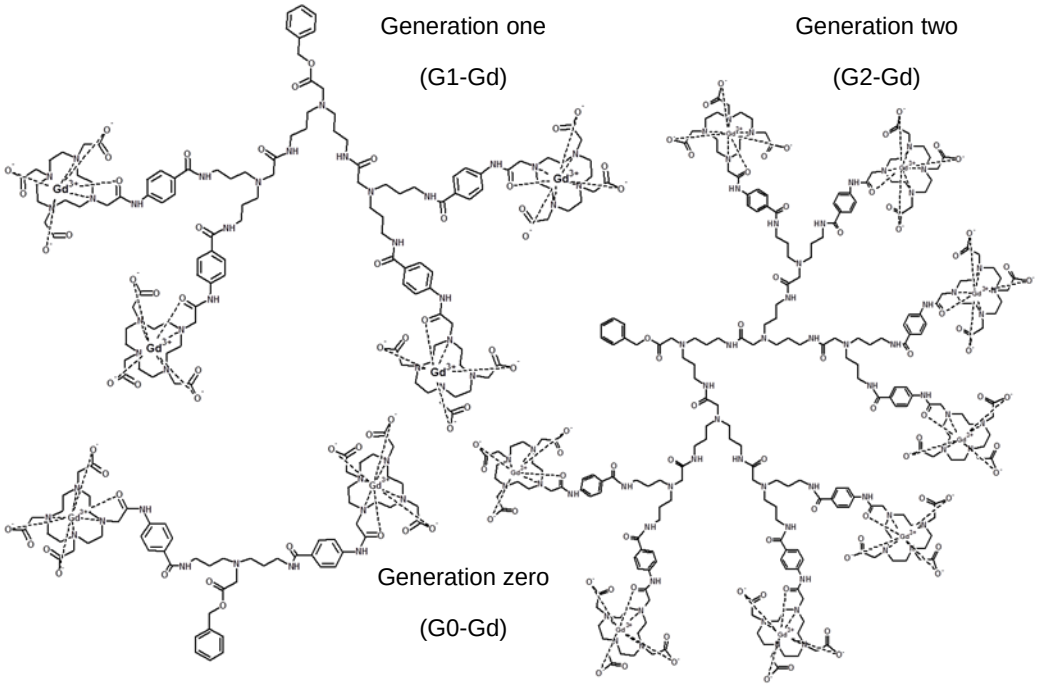

Physico-Chemical Characterisation of Chloride Transmembrane Transport using Calix[6]arene-based Receptors

G. Grauwels[1], H. Valkenier[1], L. Fusaro[2], I. Jabin[3] and K. Bartik[1]

[1] Engineering of Molecular Nanosystems, Ecole polytechnique de Bruxelles, Université libre de Bruxelles.
[2] Unité de Chimie des Nanomatériaux (CNANO), Département de Chimie, Université de Namur.
[3] Laboratoire de Chimie Organique, Faculté des Sciences, Université libre de Bruxelles.

The development of synthetic molecular receptors that can selectively bind anions and facilitate their transport through lipid bilayers is a very topical area of supramolecular chemistry, warranted by the biological importance of transmembrane anion transport. Deficiencies at the level of anion transport through biological membranes can indeed be linked to several diseases, among which cystic fibrosis is the most well-known.[1]

Calix[6]arene-based receptors exhibit unique host-guest properties, with a high degree of selectivity, toward neutral molecules, anions, metal ions, ammonium ions or contact organic ion-pairs.[2,3] Such receptors could find applications in anion transport.

We are investigating the chloride transport properties of a family of calix[6]arene compounds functionalized on their narrow rim with urea or thiourea arms using vesicles as synthetic model membranes (Fig. 1). ^{1}H and ^{35}Cl NMR are used to evaluate the binding and transport properties of the calixarene-based. Transport properties are also evaluated using a previously reported lucigenin assay.[4] Efficient transport has been observed for the compounds bearing electron-withdrawing substituents (R, R') and the transport mechanism is being investigated in more detail.

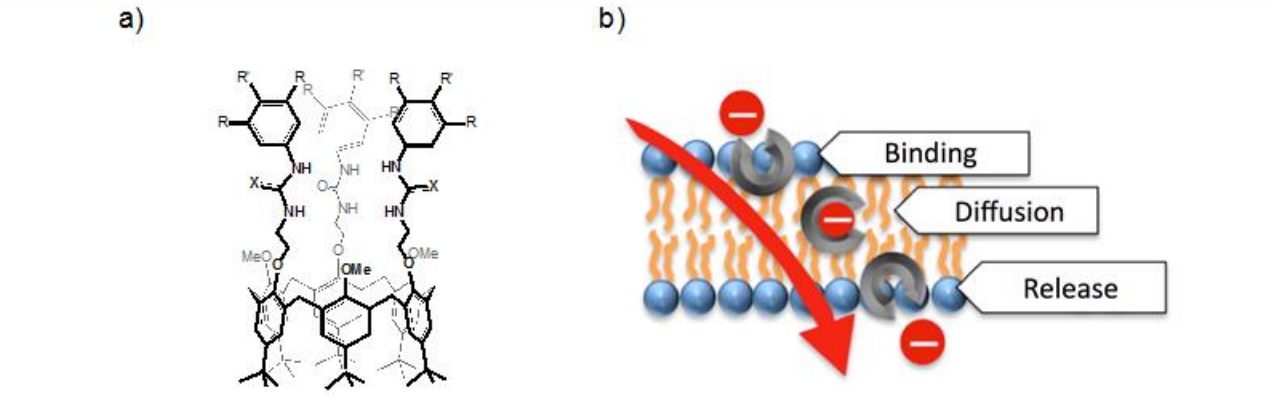

1. Ashcroft, F. in *Ion channels and disease: channelopathies*; Academic Press, San Diego (CA); 1st Ed. 1999.
2. Hamon, M., Ménand, M., Le Gac, S., Luhmer, M., Dalla, V. and Jabin, I. *J. Org. Chem.* 2008, **73**, 7067–7071.
3. Darbost, U., Rager, M.-N., Petit, S., Jabin, I. and Reinaud, O. *J. Am. Chem. Soc.* 2005, **127**, 8517–8525.
4. McNally, B. A., Koulov, A. V., Smith, B. D., Joos, J.-B. and Davis, A. P. *Chem. Commun.* 2005, **8**, 1087-1089.

Membrane Interactions of Cyclic Lipodepsipeptides

N. Geudens[1], M.N. Nasir[2], J.-M. Crowet[2], K. Fehér[1], L. Lins[2], M. Deleu[2], J.C. Martins[1] and D. Sinnaeve[1]

[1] NMR and Structural Analysis Unit, Ghent University.
[2] Centre de Biophysique Moléculaire Numérique, University of Liège, Gembloux.

Cyclic lipodepsipeptides (CLPs) are a diverse group of secondary metabolites produced by various bacteria with important biological functions, but with yet unresolved molecular mechanisms. Our previous efforts have gone towards characterizing with NMR the conformation and self-assembling properties of a collection of CLPs known as the viscosin group.[1-4] CLPs increasingly attract attention because of their antifungal and antibiotic properties through membrane permeabilization. A full understanding of their membrane interactions is essential to elucidate the exact working mechanism of CLPs.

To obtain comprehensive structural information in a membrane environment, we have used liquid-state NMR and model membrane systems, such as micelles and isotropic lipid bicelles. Like micelles, isotropic bicelles display favourable NMR relaxation properties, while possessing structural characteristics of lipid bilayers.[5] The orientation and insertion depth of CLPs in a membrane environment can be investigated using diffusion NMR and paramagnetic relaxation enhancement measurements. The latter is achieved by introducing paramagnetic probes at various locations. By introducing a water-soluble paramagnetic complex to a bicelle sample, NMR signals from nuclei closer to the aqueous phase can be identified. Adding lipid molecules with covalently linked paramagnetic radicals at various positions deliver the orientation and the insertion depth of the peptides in the bilayer. Finally, ^{31}P longitudinal relaxation measurements allow to obtain detailed information regarding the local dynamics of the lipid head groups of the bicelles.[6]

The NMR results are complemented with other experimental techniques, including fluorescence spectroscopy, circular dichroism and infrared spectroscopy. We have also performed all-atom molecular dynamics (MD) simulations of CLPs within lipid membranes, which can be confronted with the experimental NMR results.

1. Sinnaeve, D., Hendrickx, P.M. *et al.*, *Chemistry - A European Journal* 2009, **15**(46), 12653-12662
2. Sinnaeve, D., Delsuc, M.-A. *et al.*, *Chemical Science* 2012, **3**, 1284-1292
3. De Vleeschouwer, M., Sinnaeve D. *et al*., *Chemistry - A European Journal* 2014, **20**(25), 7766-7775
4. Geudens N., De Vleeschouwer M. *et al*., *ChemBioChem* 2014, **15**, 2736-2746
5. Durr, U. H., Gildenberg M. *et al*., *Chem. Rev.* 2014, **112**(11), 6054-6074
6. Bodor, A., Kover, E *et al., BBA Biomembranes* 2015, **1848**(3), 760-766

Multi-modality imaging to assess metabolic shift in tumors

M-A. Neveu[1], G. De Preter[1], N. Joudiou[1], A. Bol[2], J. R. Brender[3], K. Saito[3], S. Kishimoto[3], V. Grégoire[2], B. F. Jordan[1], M. C. Krishna[3], O. Feron[4] and B. Gallez[1]

[1] Biomedical Magnetic Resonance Research Group, Louvain Drug Research Institute, Université catholique de Louvain.
[2] Radiation Oncology Department & Center for Molecular Imaging, Radiotherapy & Oncology, Institute of Experimental and Clinical Research, Université catholique de Louvain.
[3] Radiation Biology Branch, National Cancer Institute, National Institute of Health, USA.
[4] Pole of Pharmacology and Therapeutics, Institute of Experimental and Clinical Research, Université catholique de Louvain.

Enhanced glycolysis has been recognized as a common metabolic feature of cancer. However, new evidence of oxidative activities in tumor cells has challenged this paradigm. Indeed, some tumor cells majorly rely on oxidative phosphorylation for energy production and besides the glycolytic and oxidative phenotypes, some cancer exhibits hybrid phenotypes with an amassed metabolic flexibility. All these adaptive behaviors represent major challenges for therapies. A better understanding of these processes associated with the characterization of metabolic patterns for each tumor patients would lead to the development of more efficient anti-cancer strategies.

Therefore, the objective of the work was to explore the value of different non-invasive imaging modalities to assess tumor metabolic profiles in vivo and their pharmacological modulations. We designed a multi-modality imaging project 1) to identify metabolic signature of glycolytic and oxidative tumor models and 2) to monitor the impact of metabolic modulations induced by dichloroacetate treatment and carbogen breathing. In parallel to in vitro characterizations, advanced imaging techniques including EPR oximetry, ^{13}C-hyperpolarized MRI, ^{17}O MRS and ^{18}F-FDG PET, were used to characterize oxygenation, pyruvate transformation, oxygen consumption and glucose uptake in well-established tumor models in vivo.

In vitro, the tumor models under study exhibited distinct metabolic behaviors, which was consistent with previous phenotyping studies of the tumor cell lines. However, in vivo, we were not able to discriminate the behavior of these tumor models using imaging techniques. Consequently, our study reveals major discordances between in vitro and in vivo metabolic profiles, highlighting limitations of direct translation of in vitro discoveries to the in vivo context. The absence of true correlation between in vitro and in vivo tumor models suggested the key role of local microenvironment and host cells to shape tumor features.

In conclusion, our study identified dissimilarities between in vitro and in vivo behavior of tumor models. Multimodal non-invasive imaging should be considered to identify relevant metabolic alterations in patients, which would help for anticancer treatment development.

Lanthanide (Dy^{3+}, Ho^{3+}) doped upconversion (NIR-NIR) nano-architecture as multimodel contrast agents for next generation MRI and Optical imaging

S. Biju[1], L. Vander Elst[2] and T.N. Parac-Vogt[1]*

[1] *Department of Chemistry, KU Leuven, Celestijnenlaan 200F, 3001 Leuven.*
[2] *Department of General, Organic and Biomedical Chemistry, University of Mons.*

Ever since in 1973, Lauterbur[1] proposed that the principle of nuclear magnetic resonance (NMR) can be exploited for imaging and magnetic resonance imaging (MRI) has emerged as one of the most commonly used bioimaging techniques. Even though MRI has several advantages over its counterparts (PET, SPECT and CT), like its high spatial and temporal resolution, excellent tissue penetration depth, and non-usage of radioisotopes or X-rays,[2] it is still restricted in the clinical practice to detecting disparities in magnetic properties of tissues and organs mainly because of its low contrast.[3] The introduction of MRI as a diagnostic tool, the interest in contrast agents (CA) as efficient, responsive and tissue-specific markers has grown tremendously. In a recent study, we linked a paramagnetic gadolinium(III)-chelates based on the 2-[4,7,10-tris(carboxymethyl)- 1,4,7,10-tetraazacyclododec-1-yl]acetate (DOTA) ligand to the surface of NaGdF4:Yb^{3+},Tm^{3+} upconverting nanoparticles has favorable properties for bimodal Magnetic Resonance Imaging (MRI) and Optical Imaging (OI).[4] However it has been noticed that the optimal field strength for Gd- chelates (T1) and iron oxide (T2) based CAs are below 3T.[5] But preclinical MRI studies with small animal models must provide the highest possible resolution; hence present day MRI technology heavily rely on very high field strengths (>7 T)[6]. Lanthanide ions like Tb^{3+}, Dy^{3+} and Ho^{3+} are characterized with high magnetic moments, and in particular Dy^{3+} and Ho^{3+} have very fast spin relaxation and have been shown to be very suitable as potential T_2 contrast agents at high magnetic fields. Thus here we report the synthesis, optical and magnetic properties of Dy^{3+} and Ho^{3+} containing nanoparticles with an upconverting (UC) core covered with a MRI active shell. The synthesized nanoparticles show bright green emission due to the energy migration mediated upconversion of Er^{3+} when excited at 980 nm in water medium. Furthermore, a r_2 value of 70.10 mM^{-1} s^{-1} per lanthanide(III)-ion at 500 MHz and 310 K has been shown by nanoparticles doped with 40% of Dy^{3+} in the shell. Thus the imaging agents that we developed in the present study can be considered as a novel generation of T_2 CAs as they will be effective at high magnetic fields, resulting in high resolution and better contrast of images.[7] Using the same synthetic methodology, we have now developed some NIR-NIR upconverting multimodal contrast agent based on $NaHoF_4$ nanoparticles, latest results of UC luminescence and relaxometric studies of these materials will also be discussed.

1. P. C. Lauterbur, *Nature* 1973, **242**, 190-191.
2. D. H. Geschwind and G. Konopka, *Nature* 2009, **461**, 908-915.
3. P. Verwilst, S. Park, B. Yoon and J. S. Kim, *Chem. Soc. Rev.* 2015, **44**, 1791-1806.
4. S. Carron, Q. Y. Li, L. Vander Elst, R. N. Muller, T. N. Parac-Vogt and J. A. Capobianco, *Dalton Trans.* 2015, **44**, 11331-11339.
5. P. Caravan, *Chem. Soc. Rev.* 2006, **35**, 512-523.
6. G. K. Das, N. J. J. Johnson, J. Cramen, B. Blasiak, P. Latta, B. Tomanek and F. C. J. M. van Veggel, *J. Phys. Chem. Let.* 2012, **3**, 524-529.
7. S. Biju, M. Harris, L. Vander Elst, M. Wolberg, C. Kirschhock and T. N. Parac-Vogt, RSC Adv. 2016, **6**, 61443-61448.

Mechanism of guest exchange in the cavity of a biomimetic calix[6]arene based receptor: input of 1D EXSY NMR

E. Brunetti[1,2], O. Reinaud[3], M. Luhmer[4], I. Jabin[2] and K. Bartik[1]

[1] *Engineering of Molecular NanoSystems, Ecole polytechnique de Bruxelles, ULB.*
[2] *Laboratoire de Chimie Organique, Faculté des Sciences, ULB.*
[3] *Laboratoire de Résonance Magnétique Nucléaire Haute Résolution, Faculté des Sciences, ULB.*
[4] *Laboratoire de Chimie et Biochimie Pharmacologiques et Toxicologiques, Université Paris Descartes.*

The biomimetic calix[6]arene tris-imidazole Zn(II) complex can accommodate neutral guests in its cavity, the Zn cation adopting a tetrahedral geometry (Figure 1).[1] As the Zn cation cannot be tri-coordinated, the hypothesis put forward to explain guest exchange is that an intermediate step is required, where the Zn(II) ion adopts a trigonal bipyramidal geometry and is coordinated simultaneously to the guest inside the cavity and to an *exo*-ligand outside the cavity (associative mechanism shown in Figure 2). 1D NMR EXchange SpectroscopY (EXSY) experiments were undertaken, for several guests under different experimental conditions, in order to obtain quantitative information on the exchange kinetics.[2] Results show that the guest residence time linearly depends on the concentration of water present in solution, whereas it is independent of guest concentration. This underlies the very specific role played by water as *exo*-ligand and confirms the associative mechanism, as proposed in Figure 2. This mechanism of exchange has also been confirmed with other related calix[6]arene zinc complexes.

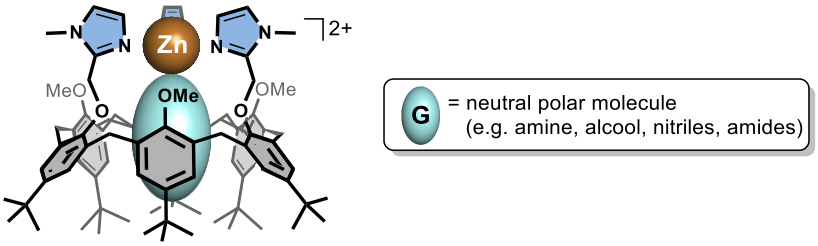

Figure 1. Structure of calix[6]arene tris-imidazole Zn(II) complex.

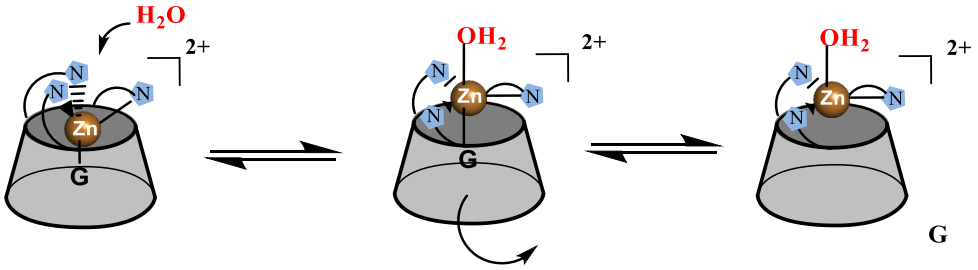

Figure 2. Proposed mechanism for guest exchange by water assistance.

1. Sénèque, O., Rager, M.-N., Giorgi, O. and Reinaud, O. *J. Am. Chem. Soc.* 2000, **122**, 6183-6189. Sénèque, O., Rager, M.-N., Giorgi, O. and Reinaud, O. *J. Am. Chem. Soc.* 2001, **123**, 8442-8443. Sénèque, O., Rondelez, Y., Le Clainche, L., Inisan, C., Rager M. –N., Giorgi, M. and Reinaud, O. *Eur. J. Org. Chem.* 2001, 2597-2604. Sénèque, O., Giorgi, O., and Reinaud, O. *Supra. Chem.* 2003, **15**, 573-580. Le Poul, N., Le Mest, Y., Jabin, I. and Reinaud, O. *Acc. Chem. Res.* 2015, **48**, 2097-2106.
2. Hu, H. and Krishnamurthy, K. *J. Magn. Reson.* 2006, **182**, 173-177.

Magnetic inequivalence in an isotope-labelled trimethyl amine : complicated yet simple spectrum or simple yet complicated spectrum?

U. le Paige[1], B. Smits[1], P. 't Hart[2], F. Lefeber[3], N. Martin[2] and H. van Ingen[1]

[1] *Macromolecular Biochemistry, Universiteit Leiden, Netherlands.*
[2] *Medicinal Chemistry and Chemical Biology, Universiteit Utrecht, Netherlands.*
[3] *NMR facility, Universiteit Leiden, Netherlands.*

In symmetrical molecules, certain nuclei are in a chemically equivalent environment, leading to an identical chemical shift. However, the scalar couplings present in such spin systems can lead to a strong magnetic inequivalence, generating several additional splittings and therefore complicating the extraction of spin resonance frequencies and scalar coupling constants. The ^{13}C-^{15}N labelled trimethyl amine gives an extreme case of such magnetic inequivalence, leading to a very unusual – but highly instructive – spectrum. In this talk are presented the results of an exact numerical simulation and the approach followed in the reconstruction of this complex system. We show that due to the large difference of magnitude between the one bond and three bonds H-C couplings, it is possible to approximate the spin system to three independent weakly coupled sub-spectra, for each set of sums of carbon spin states. The large difference of coupling constants also allows to remove all effects from the magnetic inequivalence by spin-state selective homodecoupling. The peculiar peak pattern given by this molecule and the controlled reduction to magnetic equivalence highlights the richness of NMR coupling phenomena.

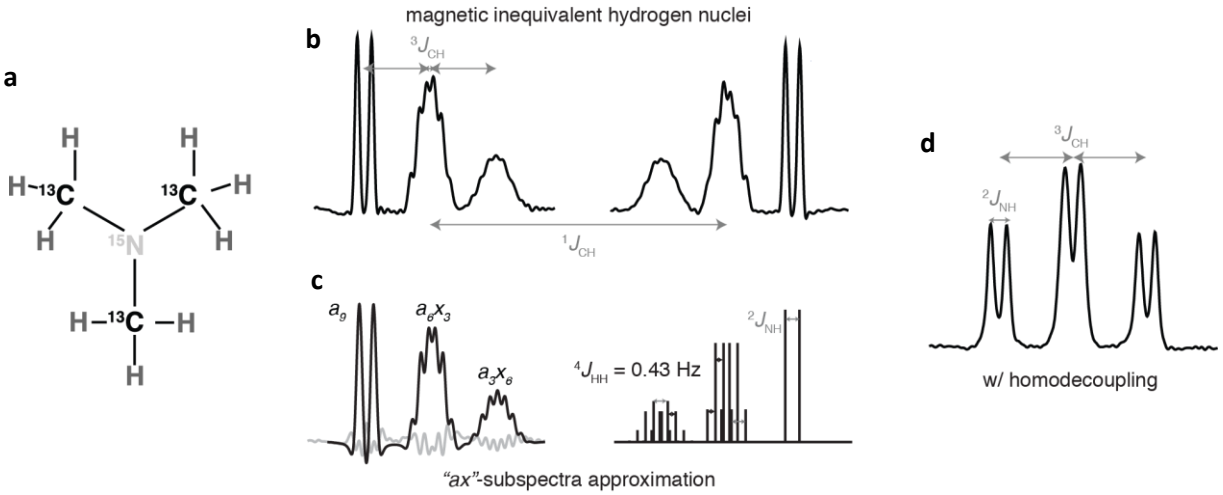

Figure 1: **a**. Representation of the isotope labelled trimethylamine. **b**. Experimental ^1H spectrum. **c**. simulated spectrum (left) and subspectral decomposition (right), with highlight of the spins systems generating the respective components. **d**. Experimental ^1H spectrum with homodecoupling applied to the opposite $^1J_{CH}$ multiplet component

Rapid protein structure determination using experimental NMR data

M. Wanko and C. Damblon

Structural Biological Chemistry Unit, Department of chemistry, University of Liege.

The knowledge of the tridimensional structure of a protein is essential to design drugs, to predict protein function and to study mechanism of protein function. 3D structure can be determined using two experimental techniques: X-Ray and NMR. However, these techniques have limitations: they are time consuming, manually intensive and sometime technically difficult. Due to these limitations, different approaches that combine the strength of computer and sparse experimental NMR data such as backbone chemical shifts, NOEs distances and residual dipolar couplings have been proposed for the determination of 3D protein structure. Among these experimental NMR data, backbone chemical shifts are the experimental NMR data that can be rapidly, easily and accurately measured. Thus different approaches that use sparse chemical shifts such as CS-Rosetta have been designed. Unfortunately, chemical shift-based 3D structure determination approaches are limited by the size and complexity of proteins (limited to molecular proteins that weight at most 15 kDa). This limitation can be understood by the fact that every folding trajectory during sampling is completely independent of every other. To overcome this limitation, additional sparse NMR data such as homology information, NOEs distances and/or RDCs are needed. **CS-HM-Rosetta** that combines incomplete chemical shifts and information derived from homologous structures have been developed in this purpose. **CS-NOE-RDC-Rosetta**, **PHAISTOS** have been also developed to guide structures determination using chemical shifts, NOEs distances and RDCs. Despite the fact that experimental data are invaluable for guiding sampling to the vicinity of the global energy minimum, for larger proteins, these data failed to guide sampling to the native minimum state. That is why, in a number of cases the improved sampling methodology makes a larger contribution than incorporation of additional experimental data. New sampling protocol named Resolution Adapted Structural RECombination (RASREC) has been therefore designed to overcome size limitation when using CS-Rosetta protocol. Unfortunately, most of these methods are not fully automated since they require manual assignment of experimental NMR data. Several automated methods such as **AUDANA, CYANA 2015, AutoNOE-RASREC-CS-ROSETTA** and **J-UNIO** that automatically assigned NOESY cross peaks, and chemical resonance assignment for **J-UNIO** have been developed. Up to now, they have not been compared together. In addition, they require expertise in computer science. Therefore, I am working toward getting fully automated approach, designed for non computer science and NMR experts that combines J**-UNIO** and **AutoNOE-RASREC-CS-ROSETTA** for rapid (4 weeks) protein 3D structure determination using unassigned backbone chemical shifts, NOESY spectra and RDCs spectra as input.

During the 15th edition of the YBMRS meeting, I will compare **CS-Rosetta, CS-RASREC-Rosetta, CS-HM-Rosetta and Homology modeling** approches based on the quality of derived 3D structures for proteins for which chemical shifts are available.

1. Shen et al. PNAS 2008, **105**, 4685–4690.
2. Lange, O. et al. *PROTEINS* 2012, **80**, 884–895.
3. Hiller, S. et al.*Top Curr Chem.* 2012, **316**, 21–48.
4. Dutta, K. et al. *J Biomol NMR* 2015, **61**, 47–53.
5. Serano, P. et al. *J Biomol NMR* 2012, **53**, 341–354.
6. Guerry, P. et al. *J Biomol NMR* 2015, **62**, 473–480.
7. Lange. O. *J Biomol NMR* 2014, **59**, 147–159.
8. Berjanskii, M. et al*. J Biomol NMR* 2015, **63**, 255–264.
9. Robustelli, P. et al*. Structure 2010* **18**, 923–933.
10. Doreleijers, F. et al*. J Biomol NMR* 2012, **54**, 267–283.
11. Berjanskii, M. et al. *Nucleic Acids Research* 2010, **38**, W633–W640.
12. Kirchner, D. K. and Güntert*,* P. *BMC Bioinformatics* 2011, **12**, 1471-2105.

Characterizing haemoglobin of the European honeybee and the malaria mosquito using optical and EPR spectroscopy

K. Nys[1], B. Cuypers[1], H. Berghmans[2], S. Dewilde[2] and S. Van Doorslaer[1]

[1] *BIMEF, Department of Physics, University of Antwerp.*
[2] *PPES, Department of Biomedical Sciences, University of Antwerp.*

The respiratory system of insects consists of trachea, which connect the inner tissues with the atmosphere. Therefore, it has been long assumed that no respiratory proteins, like haemoglobin (Hb), are present in the genome. However, in the last decades intracellular Hbs were discovered in several insects, such as the common fruit fly *D. melanogaster*.[1] Analysis of the low-spin ferric forms of this haemoglobin, using electron paramagnetic resonance (EPR), revealed a bis-histidine coordination with a large dihedral angle between the histidine imidazole planes.[2]

In order to improve our understanding of the respiratory proteins of insects, we focus here on Hb of the European honeybee *A. mellifera* (AmeHb) and of the malaria mosquito *A. gambiae* (AgaHb1). Optical absorption spectroscopy pointed out that AmeHb in its ferric form after protein purification exhibits a hexa-coordination with histidine residues binding at the proximal and distal side of the haem plane. Freshly purified AgaHb1, on the contrary, consists of an $Fe(II)O_2$ system evolving to a ferric hexa-coordinated haem form through slow temperature- and pH-dependent oxidation. Resonance Raman spectroscopy identified both AmeHb and AgaHb1 as closed conformations where the external ligand is strongly stabilised by surrounding amino acids.

Continuous wave and pulsed EPR techniques are used to probe the haem pocket structure of the ferric forms of the globins. Both Hbs feature a highly anisotropic g-tensor, which implies a large dihedral angle between the imidazole planes of the haem-ligating histidines. Furthermore, AmeHb exhibits a very unusual structure with one of the four porphyrin nitrogens differing in hyperfine and quadrupole coupling. The histidine nitrogens suffer the same inequivalency. On the other hand, in AgaHb the porphyrin nitrogens are two-by-two magnetically equivalent, what is also observed for other globins. The hyperfine and quadrupole principal values of the histidine nitrogens coordinated to the haem iron are the same within the experimental error, although the corresponding tensors are not co-axial due to the dihedral angle between the imidazole planes of the amino acid residues.

1. Burmester, T. and Hankeln, T. *J. Insect Physiol.* 2007, **53**, 285.
2. Ioanitescu, I., Van Doorslaer, S., Dewilde, S. and Moens, L. *Metallomics* 2009, **1**, 256.

Fate of intracellular iron oxides in magnetic cell tracking studies

P. Danhier[1], G. Deumer[2], N. Joudiou[1], C. Bouzin[3], P. Levêque[1], V. Haufroid[2], B.F. Jordan[1], O. Feron[4], P. Sonveaux[4] and B. Gallez[1]

[1] Louvain Drug Research Institute, Biomedical Magnetic Resonance Research Group, Université catholique de Louvain (UCL), Brussels, Belgium.
[2] Louvain Center for Toxicology and Applied Pharmacology, Université catholique de Louvain (UCL), Brussels, Belgium.
[3] Institut de Recherche Expérimentale et Clinique (IREC), IREC Imaging Platform, Université catholique de Louvain (UCL), Brussels, Belgium.
[4] Institut de Recherche Expérimentale et Clinique (IREC), Pole of Pharmacology, Université catholique de Louvain (UCL), Brussels, Belgium.

Magnetic resonance imaging (MRI) cell tracking of cancer cells labeled with superparamagnetic iron oxide (SPIO) contrast agents allows monitoring the development of metastases in preclinical models. In a MRI cell tracking study, cancer cells are first labeled in vitro with SPIO prior to their injection in vivo. We previously used this technique to track metastatic cancer cells in the mouse brain. However, MRI failed to track the long-term fate of cancer cells owing to a loss of contrast over time. We hypothesize that the decrease in MR contrast is due to the metabolism of iron oxides by macrophages.

First, 4T1 murine breast cancer cells and J774 macrophages were labeled overnight with SPIO. We next used electron paramagnetic resonance (EPR) spectroscopy and inductively coupled plasma mass spectroscopy (ICP-MS) for measuring the superparamagnetic and total iron content in cells, respectively. These experiments showed that (superparamagnetic) iron levels remained stable in 4T1 cells 5 days after SPIO labeling, whereas they decreased in J774 macrophages. In vivo MRI cell tracking of SPIO-labeled 4T1 cells evidenced a progressive loss of contrast over time. Histology studies confirmed that remaining SPIO were engulfed by tumor macrophages.

We showed that macrophages quickly metabolize SPIO in vivo. Hence, MRI cell tracking studies are only valid for the short-term monitoring of cancer cells.

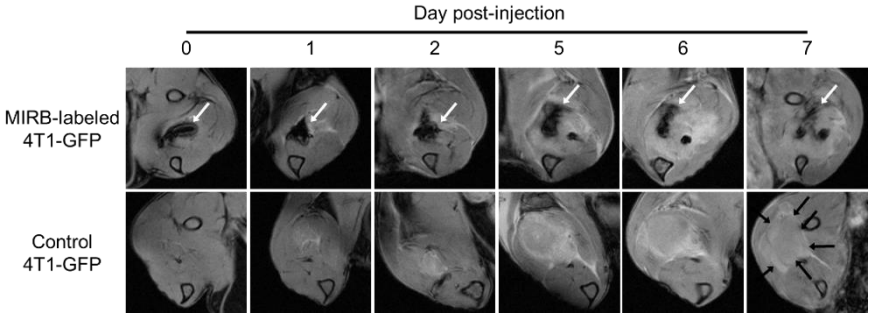

Figure 1. Loss of contrast during MRI tracking of SPIO-labeled 4T1cells.

T2*-w images of SPIO-labeled 4T1 cells (upper images), where the negative contrast due to the presence of SPIO-labeled cells over time is indicated by white arrows. T2*-w images of control 4T1 cells (lower images), highlighting the absence of signal voids due to SPIO and the apparition of a hyperintense area due to tumor growth (black arrows) (n=4)

Supported by grants from the Belgian National Fund for Scientific Research (F.S.R.-FNRS; PDR T.0107.13), the Fonds Joseph Maisin, the Communauté Française de Belgique (ARC 14/19-058) and the Télévie.

Self-Assembly of Silsesquioxane-based structures for the Design of 3D Polymeric Network

E. Carbonell, L. Fusaro and C. Aprile

Laboratory of Applied Material Chemistry (CMA), University of Namur (Unamur).

Polyhedral Oligomeric Silsesquioxane (**POSS**) nanostructures have attracted a growing interest in the scientific community due to their unique properties. Functionalized silsesquioxanes exhibit both organic and inorganic characteristics and a rigid cage-like core whose presence provides a high thermal and mechanical stability. Moreover, the organic peripheries can be easily functionalized allowing a facile tuning of the POSS properties.[1] The rational design of the organic moieties may favour specific interaction allowing the self-assembly of the POSS nanostructure. For instance, terpyridine ligands can be used for their ability to form stable interactions with a large variety of metal ions.[2] Although many functionalized POSS have been prepared, only few papers report terpyridine functionalized POSS for supramolecular self-assembly.[3] In this work, novel POSS bearing terpyridine moieties (Mono- and Octa-functionalized POSS called **M-POSS** and **O-POSS**) have been synthetized and characterized by ^{1}H, ^{13}C and ^{29}Si NMR in both solution- and solid-state (Figure 1).

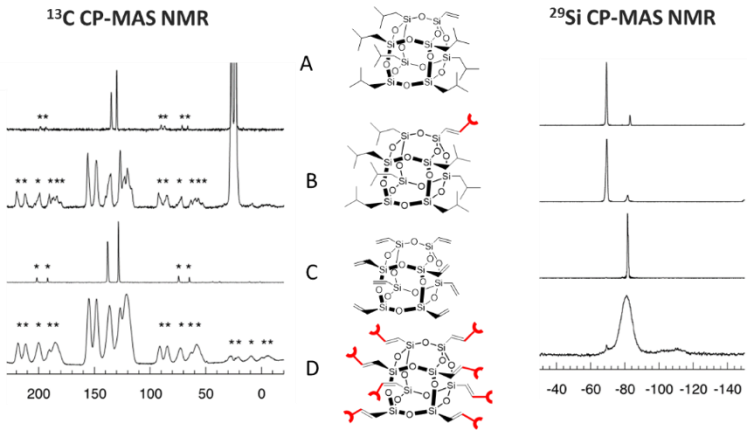

Figure 1. (A) **MVS**; (B) **M-POSS**; (C) **OVS**; (D) **O-POSS**

The self-assembly processes between M- and O-POSS with different metal ions (Zn^{2+}, Fe^{2+}) were investigated by ^{1}H NMR as well as absorption and emission spectroscopy. In the case of M-POSS, the formation of different complexes upon addition of Zn^{2+} or Fe^{2+} were observed by ^{1}H NMR. However, in the case of O-POSS, the formation of the metallopolymer was followed by the disappearance of the ^{1}H NMR signals. The obtained metallopolymers can be easily shaped in form of films and form stable gels at room temperature, being highly emissive in the case of the metallopolymer with Zn^{2+}. These materials could present potential applications in nanotechnology.[4]

1. Bivona, L.A. et al., *Catal. Sci. Technol*., 2015, **5**, 5000-5007.
2. Schubert, U. S. et al., *Chem. Soc. Rev*. 2011, **40**, 1459-1511.
3. Yam, V. W-W. et al., *J. Am. Chem. Soc*. 2014, **136**, 17910.
4. Sellinger, A. et al., *Chem. Commun*. 2005, 3700–3702.

Effects of conformational flexibility on protein function as probed by NMR spectroscopy and Molecular Dynamics simulations

K. Fehér[1], K.E. Kövér[2], Hildebrandt F.[3] and J. C. Martins[1]

[1] NMR and Structure Analysis Unit, Department of Organic and Macromolecular Chemistry, Ghent University.
[2] Department of Inorganic and Analytical Chemistry, Debrecen University, Hungary.
[3] Division of Nephrology, Harvard Medical School, Boston, MA, USA.

Protein function is intimately linked to protein flexibility as interaction with another molecule requires the protein to change its conformation. This change may be small such as rearrangement of some sidechains or maybe large involving folding. The change may take place upon binding as proposed by the induced fit theory or the conformation suitable for binding may exist already in the conformational ensemble according to the mechanism called conformation selection. It is clear that a perturbation affecting the flexibility of a protein may interfere with its function, but exactly how they are related is still debated. NMR spectroscopy and molecular dynamics (MD) simulations are ideally suited to investigate protein plasticity and flexibility at high spatial and time resolution. In this report two case studies will be presented illustrating functional dynamics in protein-protein interactions (PPI).

The first topic demonstrates the role of conformational selection over induced fit mechanism in protein-protein interactions. Anuroctoxin (AnTx), a 35-amino-acid scorpion toxin, is a high affinity blocker of voltage-gated K^+ ion channels. Since Kv1.3 channels play a key role in the activation of T lymphocytes, which are key mediators of immune responses, direct manipulation of T lymphocytes via Kv1.3 inhibition has been proposed as an effective strategy of achieving immune suppression. Thus, selective Kv1.3 blockers hold a great potential in the therapy of certain autoimmune diseases. AnTx inhibits Kv1.3, but also blocks Kv1.2 expressed in other cells of the body with similar potency. Single and double mutants of AnTx showed improved selectivity for Kv1.3 over Kv1.2 while kept high affinity for Kv1.3. The results obtained from the structures based on NMR and from MD simulations suggested that the restricted conformational space of the double substituted toxin compared to the flexible wild-type AnTx is an important determinant of toxin selectivity.[1,2] The findings may provide foundation for the possibility of designing additional, even more selective toxins targeting various ion channels.

The second topic involves prediction of consequences of single point missense mutations in the AVIL gene related to Steroid Resistant Nephrotic Syndrome on the protein level. The objective of this study is to explore the implications of the mutations on the dynamic behaviour and the structure of the protein coded by the AVIL gene, human Advillin-1 (hAvil-1). The mutations were located in comparative models built for hAvil-1in the interior of Gelsolin-Homology (GH) domain-2 and -4 in similar positions. MD simulations using enhanced sampling methods such as scaled MD, was used to accelerate the exploration of the potential energy surface in order to observe processes that require longer than nanosecond time scales. Differences in the dynamic behaviour were identified as a result of the mutations in the conformations of the GH4 and GH2 domains. The single point mutation in GH4 domain causes a displacement of the C terminal end of the acting binding α helix, while the single point mutation in GH2 domain results in the displacement of the loop after the 1st β strand and the 2nd β strand containing residues involved in the coordination of the Ca^{2+} ion. This Ca^{2+} ion was suggested to stabilize the fold of the domain. Thus, these changes in the dynamic behaviour indicate that both of these mutations have a potential to influence the function of hAvil-1.

1. Bartok, A., Feher, K., Bodor, A., Rakosi, K., Toth, G. K., Kover, K. E., Panyi, G. and Varga, Z., *Scientific Reports* 2015, **5**, 18397.
2. Fehér, K., Timári, I., Rákosi, K., Szolomájer, J., Illyés, T. Z., Bartok, A., Varga, Z., Panyi, G., Tóth G. K., and Kövér K. E. *Chemical Science* 2016, **7**, 2666 – 2673.

POSTERS

Imaging markers of response to combined BRAF - MEK inhibition in melanoma

S. Acciardo, L. Mignion, B. Gallez and B. F. Jordan

Louvain Drug Research Institute (LDRI), Biomedical Magnetic Resonance Group, Université Catholique de Louvain.

Introduction: About 50% of melanomas harbor a BRAF-activating mutation. Patients treated with the selective BRAF inhibitor vemurafenib achieve a rapid clinical benefit; however, resistance occurs in nearly every case. Multiple mechanisms of resistance to BRAF inhibition have been described, including reactivation of the MAPK pathway or activation of bypass signaling pathways. Combination therapies are thus appealing with an aim to overcome resistance. Non-invasive early markers of response are therefore needed in order to optimize combination therapies in the transition towards individualized therapy.

Methods: Nude mice bearing A375 xenografts were dosed for 7 days with either vehicle, BRAF inhibitor PLX-4032 (50 mg/kg) or the combination of PLX-4032 and MEK inhibitor GSK-112021 (0.1 mg/kg or 0.5 mg/kg). Imaging endpoints were used to evaluate tumor response, including tumor volume, diffusion-weighted MRI and MR spectroscopy.

Results: Both BRAF inhibition and combined BRAF/MEK inhibition were able to delay tumor growth, with a significantly higher delay observed for the combined inhibition under the higher trametinib dose ($p<0.0001$). Even though combined BRAFi/MEKi at the low trametinib dose did not induce a significantly longer tumor growth delay compared to the BRAFi single treatment ($p=0.8291$), total choline/water ratio was significantly decreased after five days of combined inhibition, even at the lower trametinib dose. Median apparent diffusion coefficient (ADC) had opposite trends in tumors treated with the combination, under the higher MEKi dose, and in controls ($p = 0.0470$ and 0.0292 at day 2 and 5, respectively), but none of the treated groups showed significant changes in median ADC compared to baseline. However, ADC histogram skewness and kurtosis significantly decreased following combined BRAF/MEK inhibition under the higher MEKi dose, as early as 2 days post treatment initiation (n=3, ongoing study).

Discussion/conclusion: Our findings suggest that both BRAFi and the BRAFi/MEKi combination are able to delay tumor growth in melanoma xenografts, with a significantly longer delay in tumors treated with the combination of the two inhibitors under a high MEKi dose. While choline spectroscopy is likely to highlight subtle metabolic changes that do not result in longer tumor growth delay, early effects of the combination therapy on tumor cellularity may be detected through DW-MRI as soon as two days post-treatment initiation. In particular, histographic patterns such as skewness and kurtosis of ADC distribution could be further validated as markers of response.

Future plans involve further validation of skewness and kurtosis as markers of response to combined BRAF/MEK inhibition. For that purpose, DW-MRI will be performed on BRAFi/MEKi resistant melanoma xenografts. Furthermore, metabolic markers of response, such as ^{13}C-pyruvate and ^{13}C-fumarate conversions into ^{13}C-lactate or ^{13}C-malate, will be tested on our model using ^{13}C-MRS.

Combined endogenous MR biomarkers to predict tumour basal oxygenation and response to hyperoxic challenge

T.-T. Cao-Pham, N. Joudiou, B. Gallez and B.F. Jordan

REMA laboratory, Louvain Drug Research Institute, Université catholique de Louvain, Brussels.

Hypoxia is a common feature of solid tumour which heralds a poor prognostic. Methods to counteract the negative effect of hypoxia are under evaluation. However, screening for the presence of hypoxia has not been the entry criterion to many hypoxia modification trials. Hence, to fill the gap between tumour hypoxia and the clinical routine practice, there is a need for markers of hypoxia to stratify patients, in order to determine who could benefit from an oxygen modulation.

Since tumour hypoxia varies spatially and temporally, ideal method to measure hypoxia should be non-invasive, repeatable, cost-effective and directly translatable to human trials. Oxygen sensitive endogenous MRI contrast, R_1 and R_2* are considered as potential methods as they meet these criteria. R_1 is sensitive to the oxygen dissolved in plasma and in tissue fluid while R_2* is sensitive to the ratio of the intravascular dHb/HbO_2 per tissue volume. These two endogenous MRI contrast provide us with different but complementary information regarding tumour oxygenation.

In this study, we employed two rat tumour models with distinct levels of hypoxia, 9L-glioma and rhabdomyosarcoma. Tumours were imaged for R_1 and R_2* under air and carbogen (95% O_2 and 5% CO_2) breathing conditions. Carbogen could improve the tumour oxygenation by saturation of the arterial blood.

We looked for the impact of the basal oxygenation on the amplitude of response to the carbogen challenge. Voxel-per-voxel analysis of carbogen-induced ΔR_1 and ΔR_2* map was generated for each tumour in order to assess the intra-tumoral heterogeneity. Based on the behaviour in response to the carbogen challenge, four types of voxels could be established:

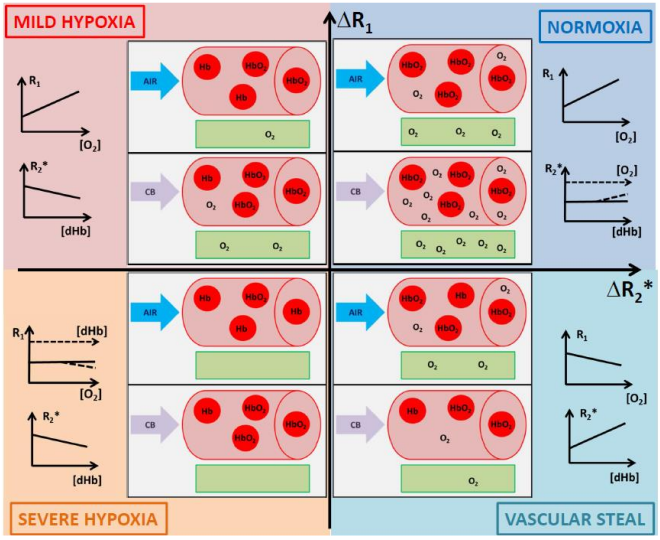

The multi-parametric analysis revealed that the proportion of the normoxic fraction in 9L-glioma tumors (25.8 ± 2.9 %) is significantly higher than in rhabdomyosarcoma tumors (11.7 ± 2.0%). Though there is no significant difference between severe hypoxic fractions of 9L-glioma (23.5 ± 3.0) and rhabdomyosarcoma (27.7 ± 3.3), the total hypoxia fraction (including severe and mild hypoxia) in rhabdomyosarcoma (76.2 ± 3.9) is significantly higher than in 9L-glioma (54.9 ± 2.7).

The results are in accordance with a previous study using 18F-FAZA and EPR oximetry. The response of the combined endogenous MRI contrast to carbogen challenge could be a useful tool to predict different fractions of tumour oxygenation.

Development of a bimodal contrast agent for MRI and PET scan

S. Chilla[1], G. Hallot[1], S. Lacroix[2], G. Doumont[2,3], S. Boutry[3], L. Vander Elst[1,3], S. Goldman[2,3], R.N. Muller[1,3] and S. Laurent[1,3]

[1] Laboratoire de RMN et d'Imagerie Moléculaire, Université de Mons, 19 Avenue Maistriau, B-7000 Mons, Belgique.
[2] Hôpital Erasme, Laboratoire de Cartographie Fonctionnelle du Cerveau, route de Lennik 808, 1070 Bruxelles, Belgique.
[3] Centre de Microscopie et d'Imagerie Moléculaire, 8 Rue Adrienne Bolland, B-6041 Charleroi, Belgique.

Medical imaging has revolutionized the world of medicine. Imaging techniques are used to look inside the body without surgery. Different types of imaging exist: structural and functional imaging. Structural imaging can locate a tumor or a lesion in a specific location of the body whereas functional imaging can help to understand the targeted cell activity.

The bimodal contrast agent developed in this work consists of three parts: the first contains a ligand complexed with gadolinium for imaging by nuclear magnetic resonance (MRI), the second part is a ligand complexed with gallium 68 for PET (positron emission tomography) imaging, and the third part is a lysine linker. Each part of the bimodal contrast agent was synthesized separately and then connected by the linker. These compounds were characterized by electrospray mass spectrometry and NMR spectroscopy.

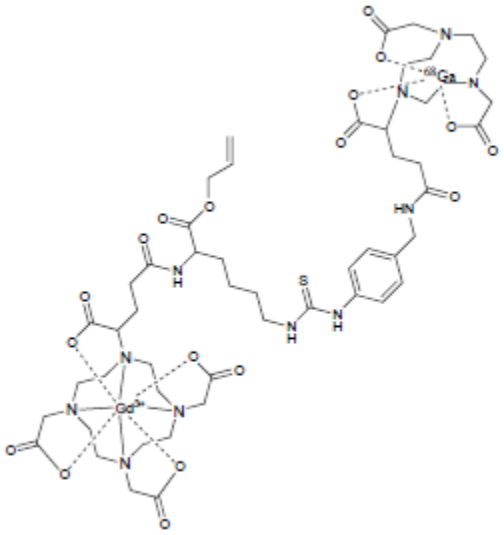

The MRI contrast agent and the bimodal molecule before complexation with gallium were characterized by measurements of relaxivity. The PET radiolabeled agent and the final product were characterized by thin layer chromatography coupled to a radioactivity detector. A first *in vivo* study was performed and has showed promising results.

Towards Lignin Valorisation: NMR Characterisation of Oxidative Cleavage Reactions using Micellar Vanadium-based Catalytic Systems

W. Denis[1,2], E. Amadio[2], G. Grauwels[1], K. Bartik[1] and G. Licini[2]

[1] *Engineering of Molecular Nanosystems, École polytechnique, Université libre de Bruxelles.*
[2] *Department of Chemical Sciences, University of Padova, Italy.*

Due to the decreasing availability of fossil fuel stocks, a global challenge is to find a green alternative to produce fuels and fine chemicals. Aromatic compounds are currently mainly produced from fossil fuels and the only biomass based alternative is lignin, a complex organic polymer present in plant cell walls that naturally contains aromatic units. In order to retrieve these units to produce high-added value chemicals, a very selective and soft degradation of lignin is necessary. Targeting the main alpha hydroxy ether bonds of lignin and perform C-C cleavage with vanadium catalysts is a possibility (Figure 1),[1] which has been studied in organic solvents in the laboratory in Padova.[2]

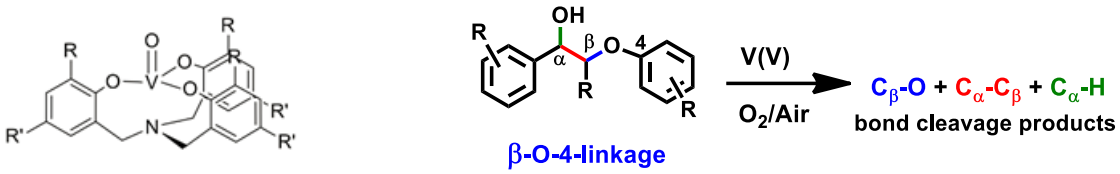

Figure 1: Structure of the vanadium(V)-amino triphenolate catalyst and possible bond cleavages of lignin model compounds

With the aim of working under "greener conditions", we are transferring these reactions into aqueous media by using micelles. The hydrophobic catalyst can indeed be incorporated into the micellar core.[3] The C-C oxidative cleavage of several lignin model compounds have been studied, under different experimental conditions, using a vanadium catalyst incorporated in dodecylphosphocholine (DPC) micelles.

Reactions were monitored by HPLC and NMR spectroscopy. Based on these results, the reactions rates were rationalised in terms of the partitioning of the substrate between the micelles and the surrounding water. Diffusion Ordered SpectroscopY (DOSY) NMR experiments were undertaken in order to determine the partition coefficients. Our results will be of help to optimise the reaction conditions when working on real lignin or lignin oils in the future.

Special acknowledgement to the Fondazione Cariparo PhD Grant for funding this research.

1. Amadio, E., Di Lorenzo, R., Zonta, C. and Licini, G. *Coord. Chem. Rev.* 2015, **301-302**, 147-162 and references therein; Hanson, K. S. and Baker, R. T. *Acc. Chem. Res.* 2015, **48**, 2037-2048 and references therein
2. Amadio, E. and Licini, G. unpublished results
3. La Sorella, G., Strukul. G. and Scarso, A. *Green chem.* 2015, **17**, 644-683

Oxygenation (measured by EPR) is a predictive marker of wound healing in diabetic mice

C. Desmet[1], G. Vandermeulen[2], V. Préat[2], Ph. Levêque[1] and B. Gallez[1]

[1] Biomedical Magnetic Resonance Research group, Louvain Drug Research Institute, Université catholique de Louvain, Brussels, Belgium.
[2] Advanced Drug Delivery and Biomaterials Research group, Louvain Drug Research Institute, Université catholique de Louvain, Brussels, Belgium.

Introduction: Impaired wound healing is a frequent complication of diabetes. Indeed, about 15 % of diabetic patients develop foot ulcers and amputation must be required in 25 % of cases as a result of healing impairments. To date, it still lacks efficient treatment to improve ulcers healing. Oxygen is known to play a key role during wound healing and hypoxia is described as a cause of wound healing impairment. EPR oximetry is a technique that allows repeated measurements of the absolute tissue pO_2 in pedicled skin flaps during the healing process. The pO_2 is determined from the linewidth of the EPR signal recorded with a biocompatible oxygen sensor such as crystals of lithium phthalocyanine (LiPc) previously implanted in the tissue.

Aims: To evaluate if LL37 (an antimicrobial peptide promoting angiogenesis) will favor wound healing in diabetic mice and to test EPR oximetry as a predictive marker of response to a treatment.

Materials and methods: LiPc crystals were implanted in the skin of male 7 and 12-week-old BKS(D)-Lepr^{db}/JOrIRj mice before the surgery. A 30 x 8 mm pedicled flap (containing the LiPc crystals) and a 4 mm diameter excisional skin wound were realized on the back of mice. The electroporation of a plasmid expressing the LL37 peptide was realized on excisional wounds and flaps. A plasmid expressing GFP was used as control. EPR signal was recorded in the flap repeatedly during the healing process. The excisional wound kinetics of closure was determined by quantification of wound area on digital photographs taken repeatedly during wound healing.

Results: After a same decrease induced by the surgery, the pO_2 slightly increased the first days after the surgery in the 7-week-old mice. Interestingly, from day 7 to day 11, pO_2 was higher in the LL37-treated group compared to the control group where pO_2 returned to very low values. Also, excisional wound kinetics of closure was faster in the treated group. In the 12-week-old mice, LL37-treated and control flaps remained hypoxic during all the monitoring. The treatment does not favor significantly the kinetics of closure of the excisional wound.

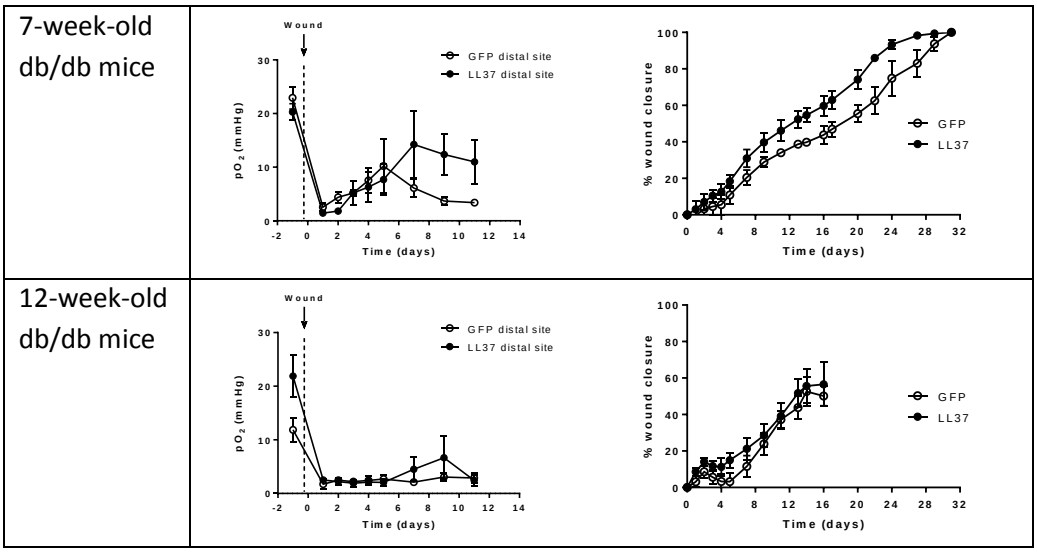

Fig 1 : pO_2 variations in the distal part of the pedicled flap (left) and excisional wound closure kinetics (right) in LL37-treated or GFP-treated (control) 7- and 12-week-old BKS(D)-Lepr^{db}/JOrIRj mice.

Conclusions: LL37 favors wound healing in 7-week-old-mice but not in 12-week-old diabetic mice.

Results obtained by EPR oximetry were consistent with the kinetics of closure of excisional wounds. EPR oximetry is a suitable tool to predict the response to a treatment.

From SiO precursor to bimodal probe : An innovative way to target inflammation?

J. Diricq[1], D. Stanicki[1], L. Vander Elst[1,2] and S. Laurent[1,2]

[1] Department of General, Organic and Biomedical Chemistry, NMR and Molecular Imaging Laboratory, University of Mons, 23 Place du Parc, B-7000 Mons – Belgium.
[2] CMMI, 8 Rue Adrienne Bolland. Aéropole de Gosselies, B-6041 Gosselies, Belgium.

Inflammation is a well-known mechanism which protects our organism from external and pathological aggressions. In its early stage, inflammation is characterized by E-selectin overexpression on vascular endothelial cells.[1] E-selectin is a cell adhesion molecule expressed on endothelial cells during inflammatory processes. This protein specifically recognizes and binds the tetrasaccharide Sialyl Lewis X ($SiLe^x$) located on the surface proteins of leukocytes. This interaction initiates leukocytes « rolling » on inflamed endothelial cells which are the first step of their strong adhesion and transmigration to the surrounding tissues. Although E-selectin plays an important role in the physiological mechanisms regulating inflammation reactions, it is now established that this protein is also heavily involved in several disorders including, among others, inflammatory and cardiovascular disorders or some cancers.

For a few years, medical imaging has been of great interest for the diagnosis of diseases. Today, the main challenge is focused on the development of combined techniques, to take advantage of their strength. In this work, we focused on the development of a bimodal probe able to target inflammation and active in both magnetic resonance imaging (MRI) and optical imaging.[2]

The structure of the bimodal probe proposed in this work consists of a silica nanoparticle with a incorporated luminescent probe, a paramagnetic complex, a hydrophilic polymer (PEG) and a mimetic of Sialyl Lewis.[3]

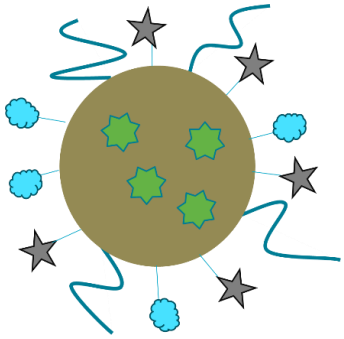

1. Lawrence M. B. and T. A. Springer, *Cell* 1991, **65**, 859-873.
2. Lipani, E. *et al.*, *Langmuir* 2013, **29**, 3419-3427.
3. Kogan, T. P. *et al.*, *Journal of Medicinal Chemistry* 1995, **38**, 4976-4984.

Mono- and bimetallic porphyrin-based complexes: what we can learn from heteronuclear NMR?

L. Fusaro[1], V. Ndoyom[2], T. Roisnel[2], V. Dorcet[2], B. Boitrel[2], and S. Le Gac[2]

[1] Département de Chimie, Université de Namur.
[2] Institut des Sciences Chimiques de Rennes, Université de Rennes 1, France.

The formation of mono-and bimetallic complexes of porphyrin ligands bearing one or two straps are investigated. The presence of an overhanging carboxylate group on the strap is responsible for the instantaneous insertion of the metal ion(s), and allows the formation of bimetallic species with unique dynamic behaviours.

First of all, the complexation of Cd(II) was studied.[1] In absence of a base, the homobimetallic complexes show both metal ions coordinated to the N-core. In presence of acetate, a metal ion is bound to the N-core of the ligand, while a second metal ion is coordinated exclusively to the overhanging carboxylate group. These metal ions exchange their coordination mode in a concerted way while staying on their respective side of the macrocycle.

Consequently, formation of homo- and heterobimetallic complexes with Cd(II), Hg(II), and Pb(II), were extensively investigated.[2] Different intra- and intermolecular dynamics were characterised, as well as a dynamic constitutional evolution which is controlled by successive addition of two chemical effectors.

Then, the sunlight-driven formation and dissociation of dynamic mixed valence Tl(III)/Tl(I) complexes was studied.[3] Tl(III) is bound on the porphyrin N-core while the Tl(I) is coordinated to the carboxylate group of the strap. The metals exchange their position symmetrically to the porphyrin plane with the Tl(III) funnelling through the macrocycle.

Finally, the spontaneous oxidation from Tl(I) to Tl(III) of a dynamic heterobimetallic Hg(II)/Tl(I) porphyrin complex was characterised.[4] Different intra and intermolecular dynamics were highlighted also in this case, with the Hg(II) funnelling trough the macrocycle and the Tl(I) in exchange between the straps.

The complexation of the different metal ions and the characterisation of different dynamics were evidenced by ^{1}H NMR spectroscopy and especially by ^{113}Cd, ^{199}Hg, ^{205}Tl, and ^{207}Pb heteronuclear NMR studies, conducted at variable temperature. In particular, the use of heteronuclear NMR has shown to provide information otherwise not accessible.

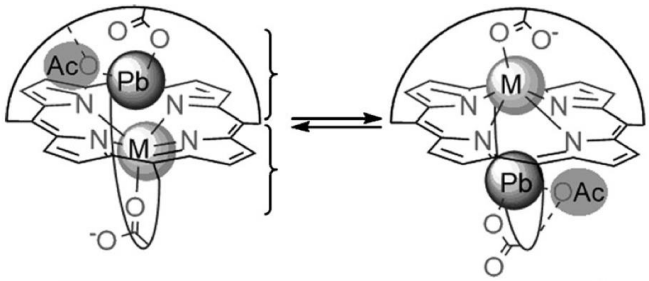

1. Le Gac, S., Fusaro, L., Dorcet, V., Boitrel, B. *Chem. - Eur. J,* 2013, **19**, 40, 13376-13386
2. Le Gac, S., Fusaro, L., Roisnel, T., Boitrel, B. *J. Am. Chem. Soc.* 2014, **136**, 18, 6698-6715
3. Ndoyom, V., Fusaro, L., Dorcet, V., Boitrel, B. Le Gac, S., *Angew. Chem, Int. Ed*. 2015, **54**, 12, 3806-3811
4. Ndoyom, V., Fusaro, L., Roisnel, T., Le Gac, S., Boitrel, B. *Chem. Commun.* 2016, **52**, 3, 517-520

The effect of a high-fat, high-sugar Western-type diet on brain volumetrics of APP-PS1 transgenic animals

K. Govaerts[1], J. Sternisa[1], J.R. Rangarajan[2], F. Van Leuven[3] and U. Himmelreich[1]

[1] *Biomedical MRI Unit, MoSAIC, KU Leuven, Leuven.*
[2] *ESAT, KU Leuven, Leuven.*
[3] *LEGTEGG, KU Leuven, Leuven.*

Introduction. Alzheimer's Disease (AD) is a devastating neurodegenerative condition, with no known cure. Many risk factors for AD correspond to diet and lifestyle, such as fat and cholesterol levels, smoking, diabetes mellitus, as well as many vascular risk factors such as atherosclerosis and ischemic stroke. Although epidemiological studies suggest that these factors may exacerbate or even instigate AD,[1] the effects of these factors in mouse models remains controversial.[2] We hypothesized that APP-PS1 transgenic mice might display AD-like symptoms such as brain atrophy more rapidly when challenged with a Western-type diet, which is high in saturated fats, cholesterol and sugar.

Methods. We imaged 7 APP.KM670/671NL (Swedish) x PS1.L166P animals (denoted APP-PS1) and 7 age-matched controls. After the initial scan session at 2 months of age, animals were given either a high-fat, high-sugar, high-cholesterol Western-type diet (n=4/group, TD88137, ssniff Spezialdiäten) or a control diet (n=3/group, CD88137, ssniff Spezialdiäten) for the remainder of the experiment. Animals were longitudinally imaged on a 9.4T Bruker Biospec small animal MRI system at 2, 4 and 6 months of age. Animals were anesthetized using a mixture of ketamine (150mg/kg), midazolam (4mg/kg) and atropine (0.5mg/kg) and subsequently intubated and mechanically ventilated. The imaging protocol was a 3D, T_2-weighted, respiratory gated RARE sequence (TR 1s, TE 12ms, RARE factor 10, resolution 0.094mm isotropic, matrix 256x160x88). Brain volumes were manually corrected after running the images through a semi-automatic segmentation pipeline.

Results and conclusion. Although all animals on a Western-type diet gained weight, the effect of this diet was less pronounced in APP-PS1 animals. While all control animals passed 50g, transgenics lagged 5-10g behind, despite all starting off around 28g at baseline. Transgenic animals showed a highly significant decrease of 3-4% in total brain volume even at 4 months of age (2mo: n.s., 4mo: p<0.0001, 6mo: p<0.001). No significant effect of diet was found, although transgenics under a Western-type diet showed slightly more severe decreases in brain volume.

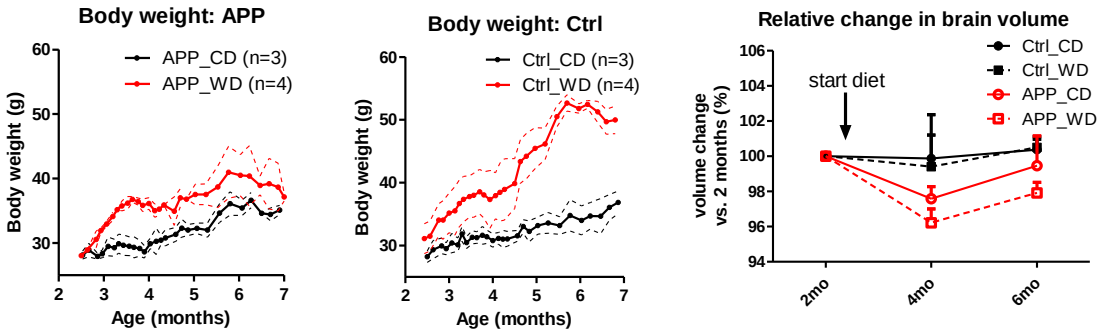

1. Kivipelto M., *Arch. Neurol. 2005*, **62(10)**, 1556-60
2. Gratuze M., *Neurobiol. Aging 2016*, **47**, 71-73

Using globins in biosensors

Z. Hafideddine[1], S. Dewilde[1] and S. V. Doorslaer[2]

University of Antwerp, Department of Biomedical Sciences, Laboratory of Protein chemistry, Proteomics and Epigenetic Signalling (PPES), Antwerp, Belgium – e-mail: zainab.hafideddine@uantwerpen.be.
University of Antwerp, Department of Physics, Biophysics and Biomedical Physics (BIMEF), Antwerp, Belgium.

Caenorhabditis elegans, a model organism, expresses 33 globins that show different expression patterns, different structures and probably also different functions. GLB-12, GLB-26 and GLB-33 have been investigated by us and have known or suspected redox functions. This implies the change of the oxidation state of the heme iron which can be detected in biosensor applications. Therefor these proteins are candidates for biosensors for the detection of small molecules like H_2O_2 and NO. Firstly, the function and redox abilities of the selected globins were investigated by overexpressing the proteins in *E. coli*. Secondly, the globins need to be immobilized on the biosensor. Both organic and inorganic materials such as nanoporous silica, titania materials and gelatines, have been proposed for protein immobilization. The properties of these matrices should avoid loss of the protein activity and leaching or degeneration of the globins. Mutations will be performed for optimizing the stability and the proteins will be purified by standard techniques. The structural and electronic properties of the globins will be studied before and after incorporation with optical absorption spectroscopy, resonance Raman (RR) and electronic paramagnetic resonance spectroscopy (EPR). Flash photolysis and stopped flow experiments are applied for the study of the ligand binding to the heme groups.

Clustering of iron oxide nanoparticles into poly(ethylene oxide)-block-poly(ε-caprolactone) nanoassemblies as ultrasensitive MRI probes

A. Hannecart[1], D. Stanicki[1], L. Vander Elst[1, 2], L. Mespouille[3], R. N. Muller[1, 2] and S. Laurent[1, 2]

[1] NMR and Molecular Imaging Laboratory, General, Organic and Biomedical Chemistry Department, University of Mons.
[2] Center for Microscopy and Molecular Imaging, Charleroi.
[3] Laboratory of Polymeric and Composite Materials, University of Mons.

Recently, polymer vesicles called polymersomes have emerged as promising nanocarriers. Several studies have reported the formation of poly(ethylene oxide)-block-poly(ε-caprolactone) (PEO-b-PCL) based vesicles due to their high potential for biomedical applications. However, to our knowledge, the incorporation of ultrasmall superparamagnetic iron oxide nanoparticles (USPIO) into these PEO-b-PCL vesicles has not yet been described.

This work reports the self-assemby of PEO2000-b-PCL12650 copolymers with USPIO (Fig. 1). PEO2000-b-PCL12650 was chosen as amphiphilic copolymer because PEO block is biocompatible and prolong the circulation time of nanoparticles in vivo whereas PCL block is biodegradable. Moreover, PEO2000-b-PCL12000 copolymers have been reported to form vesicles.[1,2]

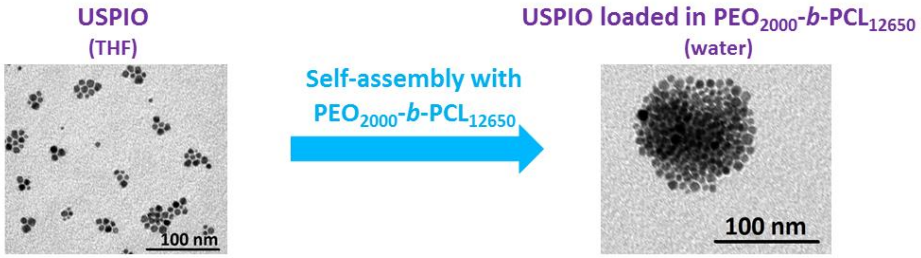

Figure 1. Clustering of USPIO into well-defined PEO_{2000}-*b*-PCL_{12650} nano-assemblies

USPIO were synthesized by the thermal decomposition method (magnetic core size of 4.2 nm and 7.5 nm) and self-assembly of PEO_{2000}-*b*-PCL_{12650} with USPIO was performed by nanoprecipitation. Polymeric nanoparticles with diameters close to 100 nm and a high USPIO content were formed as shown by dynamic light scattering (DLS), transmission electron microscopy (TEM) and cryo-TEM. These nanoassemblies are characterized by very high r_2/r_1 ratios (at 20 and 60 MHz) which makes them highly promising canditates as T_2-contrast agents for magnetic resonance imaging (MRI). The size of USPIO entrapped in PEO-*b*-PCL nanoassemblies has a strong impact on their magnetic properties. Indeed it affects both their longitudinal and their transverse relaxivities and thus their magnetic resonance imaging (MRI) sensitivity.

The next steps in further studies will be the incorporation of an anti-cancer drug into these nanocarriers and the attachment of an active targeting group such as an RGD-containing peptide to their surfaces.

1. Ghoroghchian, P. *et al*., *Macromolecules* 2006, **39(5)**, 1673-1675.
2. Adams, D. *et al., Soft Matter*. 2009, **5(16)**, 3086-3096.

Synthesis and characterisation of fluorinated paramagnetic contrast agents for their use in ^{19}F MRI

E. Hequet [1], C. Henoumont [1], R. Muller [1,2], L. Vander Elst [1,2] and S. Laurent [1,2]

[1] *General, Organic and Biomedical Chemistry Department, Nuclear Magnetic Resonance (NMR) and Molecular Imaging Laboratory, University of Mons, 7000 Mons, Belgique.*
[2] *CMMI – Center for Miscroscopy and Molecular Imaging, 6041 Gosselies, Belgique.*

Medical imaging is a dynamic area of research whose the goal is the elaboration of more efficient contrast agents. Those agents need to be improved to optimize the detection of affected tissues such as cancers or tumours while decreasing the injected quantity of agents.

The paramagnetic contrast agents containing fluorine atoms can be used both on proton and fluorine MRI. This research field is therefore promising thanks to the ability to map the anatomy by ^{1}H MRI and locate exactly the agents by ^{19}F MRI. In this domain, one of the challenges is to synthesize a molecule containing several chemically equivalent fluorine atoms characterized by a short relaxation time to allow the record of fluorine MRI images in good conditions.

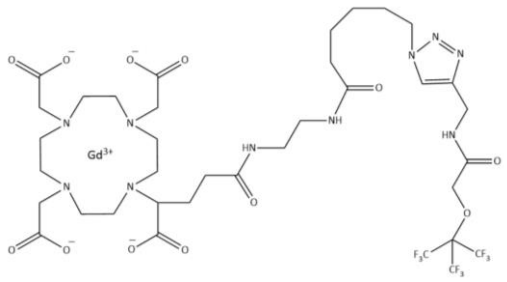

Until now, a compound containing a paramagnetic ion and fluorine atoms has been synthesized by a cycloaddition reaction between two previously synthesized products.

In a first time, a derivative of DOTAGA macrocyclic ligand has been synthesized. This macrocycle has been obtained by a multistep synthesis during which an azide function was added. Then, the ligand has been complexed with a lanthanide ion, the gadolinium which is paramagnetic.

Then, a nonafluorinated compound containing an alkyne function has been synthesized in order to allow the use of the contrast agent in fluorine MRI.

Finally, these two molecules were combined via a Click Chemistry reaction.

The fluorinated paramagnetic contrast agent has been characterized by relaxometry which shows an increase of the agent efficiency in comparison with the parent compound Gd-DOTA.

Finally, a ^{19}F NMR study has shown a significant decrease of the fluorine-19 relaxation time (from about 25 ms for the single molecule to about 10 ms for the molecule conjugated to the paramagnetic macrocycle) which is promising for a future use in ^{19}F MRI.

It will be now essential to perform MRI ^{19}F *in vitro* and *in vivo* tests to evaluate the diagnosis potential of the synthesized contrast agent.

Investigation of the effects due to the insertion of a polyQ tract increasingly long on the structure and dynamic of BlaP using NMR spectroscopy

J. Kay[1], T. Banelli[2], M. Vuano[2], D. C. Thorn[1], S. Preumont[1], F. Fogolari[2], C. Damblon[3], A. Corazza[2] and M. Dumoulin[1]

[1] *Centre for Protein Engineering, University of Liège, Liège*
[2] *Dipartimento di Scienze Mediche e Biologiche, Università di Udine, I-33100 Udine, Italy*
[3] *Institute of Chemistry, University of Liège, Liège*

Polyglutamine (polyQ) diseases, which include the well-known Huntington's disease, arise from an anomalous expansion of a polyQ tract within proteins specific to each disease[1]. When the length of this polyQ tract is higher than a characteristic threshold (~35-45Q), it becomes pathogenic by triggering the aggregation of disease-associated proteins into amyloid fibrils which are deposited in neurons as nuclear inclusions and lead to the death[2]. Although the polyQ repeat was thought to be the only determinant factor that mediates the aggregation, recent studies have demonstrated that non-polyQ regions of these proteins play also a significant role, either preventive or facilitative, into the aggregation process[3-4]. In order to better understand the complex interplay between the ability of the polyQ tract to mediate the aggregation and the modulating effect of non-polyQ regions, we engineered in our lab chimeric proteins by inserting at two positions (i.e. 197 and 216) a polyQ tract of various lengths (i.e. 23Q, 30Q, 55Q and 79Q) into the β-lactamase BlaP from Bacillus licheniformis 749/C[5]. Both sets of BlaP chimeras recapitulate the aggregation behaviour of disease-associated proteins: indeed there is a repeat threshold length above which the chimeras readily assemble into amyloid fibrils and the rate of assembly increases with polyQ length. While having little impact on the overall structure, the location of the polyQ tract affects the tertiary structure, enzymatic activity, unfolding cooperativity and stability of the chimeric proteins, and more importantly, it significantly affects their aggregation propensity. Indeed, the 216 chimeras exhibit a significantly higher fibril-forming propensity than their 197 counterparts[6]. The aim of my work was to use NMR to investigate, at the molecular level, the effects of polyQ insertions on the structure and the dynamics of BlaP, in order to better understand the differences in the aggregating properties of the two sets of chimeras. First, I assign 98.5% of the backbone 1H-15N correlations in the 2D-HSQC spectrum of BlaP216Q0 using a series of triple resonance NMR experiments. Then, the regions of BlaP affected by the insertion of the dipeptide PG at either position 197 or 216 were identified by comparing their respective [1H-15N] 2D-HSQC spectrum with that of the wild-type. This dipeptide PG has been introduced within the gene of BlaP, at these two specific positions, to allow poly(CAG) sequence insertion. Changes in the chemical shift of each residue due to the PG insertion were therefore determined. In both cases, the perturbations are essentially located around the insertion site (i.e. helix H8 for BlaP197Q0 and helix H9 for BlaP216Q0); they are, however, more significant when the dipeptide is inserted at position 216 than at position 197. Perturbations also occur in the three left-located helixes (i.e. H3, H4 and H9) that seem to laterally propagate the perturbation because of side chains interactions. In order to investigate eventual changes in the dynamic of BlaP upon the insertion of the dipeptide PG, real time hydrogen/deuterium exchange experiments were carried out. The preliminary analysis indicates that the dynamics of BlaP is more perturbed by the insertion at position 216 than at position 197; this result is in agreement with the lower thermodynamic stability of this chimera. Finally, the perturbations due to the presence of a polyQ tract increasingly long were also investigated. Globally, polyQ insertion at position 197 induces perturbations essentially located in the α-domain of BlaP while the perturbations due to insertion at position 216 are located in both domains. For both sets of chimera, the longer the polyQ, the farther are the perturbations on the surface of BlaP. These differences may explain the different aggregation propensity of the two sets of chimeras.

1. Hands, S. L. and Wyttenbach, A,. *Acta Neuropathol.* 2010, **120**, 419.
2. Orr, H. T., Zoghbi, H. Y. Annu,. *Rev. Neurosci,* 2007, **30**, 575.
3. Robertson, A. L. and Bottomley, S. P., *Curr. Med. Chem.* 2010, **17**, 3058.
4. 4: Wetzel, R., *Journal of molecular biology* 2012, **421**, 466.
5. Scarafone, N., Pain, C., Fratamico, A., Gaspard, G., Yilmaz, N., Filee, P., Galleni, M., Matagne, A. and Dumoulin, M., *PloS One* 2012, **7**, e31253.
6. Thorn, D., Pain, C., Huynen, C., Preumont, S., Duez, C., Brisotto, G., Matagne, A., Dumoulin, M. and Scarafone, N. In preparation.

Is it possible, that a Lewis acid has revolving acid strengths?

B. Kovács[1], É. Dorkó[2], B. Kótai[2], A. Domján[2] and T. Soós[2]

[1] NMR and Structure Analysis Unit, Vakgroep Organische Chemie, Universiteit Gent.
[2] Hungarian Academy of Sciences, Research Centre for Natural Sciences, Institute of Organic Chemistry, Budapest, Hungary.

In 1923, Gilbert N. Lewis suggested that an electron-pair donor be classified as a base and an electron-pair acceptor be classified as acid. The extent of the interaction between a Lewis acid and a Lewis base is controlled by at least two internal factors: electronic and steric. Bronsted acidity can be assessed unequivocally, since it reflects the aim for a transfer of a "tiny" proton; thus, usually it can be derived by taking only electronic effects into account. The quantification of Lewis acidity is less straightforward: the aim for electron-pair acceptation is influenced by the sterical relations between the reactants. Is it possible, that a Lewis acid has various acid strengths related to the same base? Considering the concept of Lewis acidity, if the Lewis adduct manifests in distinct conformations with different stabilities, distinct Lewis acidity values can be derived to a single molecule.

The idea of Frustrated Lewis pair (FLP) chemistry is based on the notion that combinations of Lewis acids and bases that are sterically prevented from forming classical Lewis acid–base adducts have Lewis acidity and basicity available for interaction with a third molecule.[1] Previous experiments showed[2] that (somewhat even water tolerant) asymmetrically substituted triaryl boranes (Figure 1) were able to serve as catalysts for the hydrogenation of imines. There is an apparent connection between the Lewis acid strength and the catalytic efficiency, since after the heterolytic dissociation of the H_2, the hydride ion clinches to the borane. With the application of piperidine as a model base, our goal was to demonstrate the multifarious conformations of the adducts, thus the probable multifarious Lewis acidities and catalytic efficiencies of each borane.

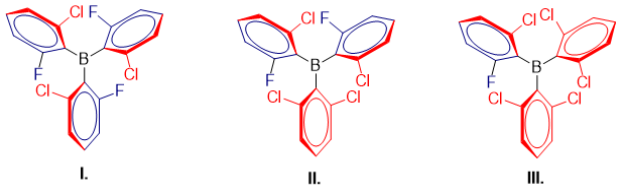

Figure 1: boranes with asymmetrically substituted aryl rings

To discover the possible structures of each complexes, a Monte Carlo conformational search was followed by *ab initio* (DFT/B3LYP-D3) geometry optimization. NMR experiments confirmed the theoretical predictions: the borane–piperidine adducts adopt to several conformations indeed. The identification of those was based on the comparison of calculated (DFT/B3LYP-D3) and experimental 19F spectra. Moreover, ^{19}F-^{1}H HOESY measurements supported the suggested assignments. Afterwards, ^{19}F DOSY experiments not only showed the differences for the hydrodynamic radii of the boranes in complexed and in non-interacting forms, but also revealed the presence of the "frustrated" state. In addition, the chemical and conformational exchanges of the observed forms were also indicated (^{19}F 2D EXSY). The latter results mean that along with the boranes possess distinct Lewis acid strengths related to the same base, these values even revolve on the timescale of the experiments.

1. Stephan, D. W., *Acc. Chem. Res.* 2015, **48**, 306-316.
2. Dorkó É. *et al.*, unpublished.

Kinetic studies of phosphoester hydrolysis promoted by a dimeric tetrazirconium(IV) Wells-Dawson polyoxometalate by NMR spectroscopy

T. K. N. Luong[1], P. Shestakova[2] and T. N. Parac-Vogt[1]

[1] Department of Chemistry, KU Leuven, Heverlee.
[2] Institution of Organic Chemistry with Centre of Phytochemistry, Bulgarian Academy of Sciences, Sofia, Bulgaria.

The detailed kinetic study of catalytic hydrolysis of a phosphoester bond in the DNA-model substrate 4-nitrophenyl phosphate (NPP) promoted by Zr^{IV}-substituted Wells-Dawson type polyoxometalate $Na_{14}[Zr_4(P_2W_{16}O_{59})_2(\mu_3\text{-}O)_2(OH)_2(H_2O)_4]\cdot 57H_2O$ (ZrWD 4:2) was followed by means of ^1H and ^{31}P NMR spectroscopy. The hydrolytic reaction proceeded with a rate constant of 8.44 (±0.36) × $10^{-5}s^{-1}$ at pD 6.4 and 50 °C, representing a 300-fold rate enhancement in comparison with the spontaneous hydrolysis of NPP (k_{obs} = 2.81 (±0.25) × 10^{-7} s^{-1}) under the same reaction conditions. The ZrWD 4:2 was also active towards hydrolysis of the more stable DNA-model substrate bis(4-nitrophenyl) phosphate (BNPP) and the RNA model substrate 2-hydroxypropyl-4-nitrophenyl phosphate (HPNP). The pD dependence profile of k_{obs} shows that the rate constants for NPP hydrolysis decrease significantly when the pD values of the reaction mixtures increase. The formation constant (K_f = 190 M^{-1}) and catalytic rate constant (k_c = 6.40 × 10^{-4} s^{-1}) for the NPP-ZrWD 4:2 complex, activation energy (E_a) of 110.15 ± 7.06 kJ mol^{-1}, enthalpy of activation ($\Delta H^{\ddagger}$) of 109.03 ± 6.86 kJ mol^{-1}, entropy of activation ($\Delta S^{\ddagger}$) of 15.20 ± 2.49 J mol^{-1} K^{-1}, and Gibbs activation energy ($\Delta G^{\ddagger}$) of 104.32 ± 6.09 kJ mol^{-1} at 37 °C were calculated from kinetic studies. The recyclability of ZrWD 4:2 was examined by adding an extra amount (5.0 mM) of NPP twice to a fully hydrolyzed mixture of 5.0 mM NPP and 1.0 mM ZrWD 4:2. The interaction between ZrWD 4:2 and the P–O bond of NPP was evidenced by a change in the ^{31}P chemical shift of the ^{31}P atom in NPP upon addition of ZrWD 4:2. Based on ^{31}P NMR experiments and the kinetic studies, a mechanism for NPP hydrolysis promoted by ZrWD 4:2 has been proposed.[1-4]

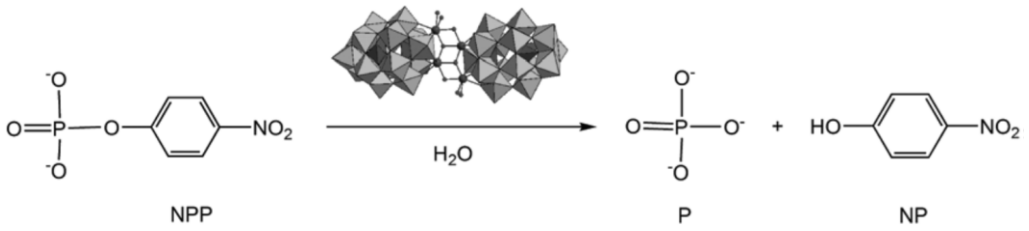

1. Luong T. K. N., Shestakova P. and Parac-Vogt T. N., *Dalton Trans.* 2016, **45**, 12174-12180.
2. Luong T. K. N., Shestakova P., Mihaylov T. T., Absillis G., Pierloot K. and Parac-Vogt T. N., *Chem. Eur. J.* 2015, **21**, 4428-4439.
3. Luong T. K. N., Absillis G., Shestakova P. and Parac-Vogt T. N., *Eur. J. Inorg. Chem.* 2014, **2014**, 5276-5284.
4. Luong T. K. N., Absillis G., Shestakova P. and Parac-Vogt T. N., *Dalton Trans.* 2015, **44**, 15690-15696.

Application of MOFs as Heterogeneous Catalysts for Hydrolysis of Peptides

H. G. T. Ly[1], G. Fu[2], D. De Vos[2] and T. N. Parac-Vogt[1]

[1] Department of Chemistry, Laboratory of Bioinorganic Chemistry, KU Leuven.
[2] Centre for Surface Chemistry and Catalysis, KU Leuven.

Selective hydrolytic cleavage of the peptide bond in proteins is one of the most important procedures in analytical biochemistry and biotechnology applications, frequently used for protein structure/function/folding analysis, protein engineering, and target-specific protein-cleaving drugdesign.[1] However, this is a challenging task due to the extreme inertness of the peptide bond, with an estimated half-life of up to 600 years under physiological pH and temperature.[2] Several proteolytic enzymes are available for this purpose, but they often cleave proteins into too many fragments that are too short to be reliably matched to the intact protein. Therefore, chemical reagents emerged as an attractive alternative to proteolytic enzymes. We have shown that Zr(IV)-substituted polyoxometalates (POMs) efficiently hydrolyze unactivated amide bonds in dipeptides, oligopeptides, and proteins, and the mechanism of these reactions has been investigated in detail.[3] The superior reactivity of Zr(IV)-substituted POMs towards peptide bond hydrolysis was confirmed in our lab and has been explained by large coordination numbers, flexible geometries, oxophilicity and increased Lewis acidity of Zr(IV).[3] Despite the successful application of Zr(IV)-substituted POMs for the cleavage of peptide bonds, the recycling of catalysts and purification of products remain problematic. The catalyst often causes formation of precipitates in the reaction mixture containing proteins, thereby preventing the use of mass spectroscopic techniques to identify fragmentation patterns. Therefore, the development of zirconium metal-organic frameworks (MOFs) as heterogeneous catalysts that are able to hydrolyze peptide bonds and can be easily removed from the reaction mixtures and recycled would greatly advance the potential of using artificial metalloenzymes in the fields of proteomics and biotechnology. In this study, several Zr-MOFs (UiO-66, UiO-66/TFA, NU-1000, and MOF-808) were synthesized and for the first time applied as heterogeneous catalysts for the hydrolysis of peptide bonds in a series of dipeptides. The hydrolysis of various peptides by MOFs was studied by ^{1}H NMR spectroscopy. Their catalytic activity towards peptide bond hydrolysis was shown to be excellent through a broad pD range of 4 to 10. A complete hydrolysis of 2.0 mM Gly-Gly by 2.0 µmol of MOF-808 was obtained after 6 hours, while no hydrolysis of Gly-Gly was observed after 7 months in the absence of MOFs. This represents a significant acceleration as compared to the uncatalyzed reactions. The stability of MOFs was found to be complete under hydrolytic conditions both in the presence and in the absence of the substrates, which was confirmed by powder XRD and FT-IR spectroscopy.

1. Grant, K. B. and Kassai, M., *Curr. Org. Chem.* 2006, **10**, 1035.
2. Radzicka, A.and Wolfenden, R. J., *Am. Chem. Soc.* 1996, **118**, 6105.
3. Absillis, G. andParac-Vogt, T. N. *Inorg. Chem.* 2012, **51**, 9902. Ly, H. G. T., Absillis, G. and Parac-Vogt, T. N. *Eur. J. Inorg. Chem.* 2015, **2015**, 2206. Ly, H. G. T., Absillis, G. and Parac-Vogt, T. N. *New J. Chem.* 2016, **40**, 976. Ly, H. G. T., Absillis, G., Janssens, R., Proost, P. and Parac-Vogt, T. N. *Angew. Chem. - Int. Ed.* 2015, **54**, 7391.

Influence of the Electrode Material on the Electrochemical Stability of an Imidazolium-based Ionic Liquids by NMR Spectroscopy

R. Michez[1], J. Vander Steen[1,2], Th. Doneux[1], C. Buess-Herman[1] and M. Luhmer[2]

*[1] Service de **CH**imie **AN**alytique et chimie des **I**nterfaces (CHANI), Université libre de Bruxelles.*
*[2] Laboratoire de **R**ésonance **M**agnétique **N**ucléaire **H**aute **R**ésolution (RMN-HR), Université libre de Bruxelles.*

During the last decades, ionic liquids have received increasing attention within the scientific community and particularly amongst the electrochemists. Imidazolium based ionic liquids, which are known for their high ionic conductivity, their wide electrochemical window and their relatively low viscosity at room temperature, appear to be good electrolytic supports for various electrochemical processes such as metal deposition or electrocatalysis.

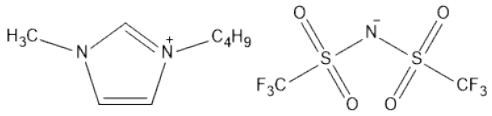

Chemical structure of the ionic liquid [BMIm][NTf_2]

$BMIm^+$ = 1-butyl-3-methylimidazolium, NTf_2^- = bis(trifluoromethanesulfonyl)imide

Little is known about the cathodic decomposition of imidazolium based ionic liquids and the stability of the ionic liquid was first investigated at a gold electrode. Long-duration electrolysis experiments of deoxygenated [BMIm][NTf_2] were performed at controlled potentials. Both the gas and liquid phases were analysed by chromatographic techniques and the composition of both the anolyte and catholyte was investigated by ^{19}F and ^{1}H NMR spectroscopy.

The present communication mainly focuses on the ^{1}H NMR analyses of the cathodic medium. Carbene formation could be indirectly evidenced because it gives rise to proton exchange with the $BMIm^+$ cation. Besides, several additional signals ascribable to the reduction of the $BMIm^+$ cation were detected and the structure of the reduction products could be elucidated thanks to various one- and two-dimensional NMR experiments, including measurements of relative diffusion coefficients. The outputs could be quantified and were found to nicely account for the total consumed charge.

Similar electrolysis experiments were performed on various electrodes (Au, Cu, Pt, Hg). The proportions of the reduction products were found to vary consistently with the expected hydrogen-atom adsorption ability of the electrode material, providing valuable information on the mechanism of cathodic decomposition of [BMIm][NTf_2].

Acknowledgement: This project is supported by a PDR-FNRS grant (BE) n° T.0090.130. R. Michez thanks the FRIA for his PhD fellowship

Design of An Effective Bimodal Diamond-based Nanoprobe for Biomedical Purposes

S. Montante[1], R. N. Muller[1,2], L. Vander Elst[1,2] and S. Laurent[1,2]

[1] Nuclear Magnetic Resonance and Molecular Imaging Laboratory, University of Mons.
[2] Center for Microscopy and Molecular Imaging, Charleroi.

The popularity of nanodiamonds has risen over the last few years because they have proved to be safe, biocompatible and significantly less toxic than other well-known carbon nanomaterials.[1] According to some studies, diamond nanoparticles seem to be a good candidate for biomedical purposes and more precisely as a tool for therapeutic and diagnosis applications in the medical imaging context.[2,3]

The main goal of this work is to validate an effective bimodal diamond-based nanoprobe for medical imaging techniques and specific of apoptosis. The functionalization of the platform involves the grafting of an optical agent (an amine-derivative of rhodamine), an apoptosis-specific vector (TLVSSL or E3 peptide), and a paramagnetic contrast agent (an amine-derivative of Gd-DOTA). The benefit of this multifunctional platform is the alliance of properties of magnetic resonance imaging (MRI) and optical imaging (OI) in terms of high spatial resolution and high sensitivity.

In this work, an annealing process has been employed to saturate the surface in a uniform way with carboxylic acid groups. The carboxylated diamond platform (n-COOH) is the starting material which enables a high surface loading of specific molecules for biomedical applications. The atomic distribution of the n-COOH surface was analyzed by XPS to define the efficiency of the oxidation method. The quantitative determination of surface carboxyl groups added by the thermal treatment was performed by conductimetric titration measurements.[4]

Parallel to the surface uniformity and the dispersion of nanoparticles in aqueous solution, a paramagnetic gadolinium complex (Gd-DOTA-NH_2) has been synthesized in order to make the nanosystem active in MRI. The intermediate products of the synthesis have been characterized by mass spectrometry and NMR techniques. The relaxivity properties of the final complex were studied at 20 and 60 MHz and compared to the commercial complex, the Gd-DOTA.

The successive couplings of the molecules of interest (fluorochrome, peptide, paramagnetic complex) with the carboxylated platform were performed in water via an EDC(/NHS)-coupling process. After intensive purification by dialysis, the efficiency of the new active and specific diamond nanoprobe for apoptosis as bimodal agent was assessed in terms of relaxometric properties (20 and 60 MHz) and in vitro studies.

1. Zhang, X. et al., *Toxicol. Res.* 2012. **1(1)**, 62-68.
2. Manus, L.M. et al., *Nano letters* 2009. **10(2)**, 484-489.
3. Chow, E.K. et al., *Sci. Transl. Med*. 2011. **3(73)**, 1-10.
4. Schmidlin, L. et al. *Diam. Relat. Mater.*, 2012. **22**, 113-117.

Analysis of the five-membered ring pucker of β- and γ-fluorinated prolines by means of NMR spectroscopy and pseudorotation theory

E. Ottoy[1], G. J. Hofman[2], J. C. Martins[1], B. J. Linclau[2] and D. Sinnaeve[1]

[1] Department of Organic and Macromolecular Chemistry, Ghent University, Ghent.
[2] Department of Chemistry, University of Southampton, Southampton, United Kingdom.

Introducing fluorine in proline enables modulating its conformational properties, which is useful to study the structure-function relation of proline within biomolecules.[1] There are two defining aspects of the proline conformation: the five-membered ring pucker, and the ratio between peptide bond *trans* and *cis* rotamers.[2] Fluorine substitutions influence both these aspects by means of stereoelectronic effects, such as the so-called *gauche* effect.[3]

We will present the analysis of the ring puckers of seven (fluoro)proline analogues in both chloroform and water using NMR spectroscopy: Pro, (4*R*)-FPro, (4*S*)-FPro, 4,4-F_2Pro, (3*R*)-FPro, (3*S*)-FPro or 3,3-F_2Pro. These are studied as Ac-X-OMe derivatives. The first three analogues are well-known in terms of their puckering behaviour [4] and are used to validate our methodology, while the puckering preferences of the latter four are less well-known. The ring pucker can be determined separately for the *trans* and the *cis* isomers, as these are in slow exchange on the NMR time-scale. The analysis occurs through analysis of the vicinal ^{1}H-^{1}H and ^{1}H-^{19}F couplings. For this, the recently developed PSYCHEDELIC experiment was used, which allows straightforward extraction of ^{1}H-^{1}H and ^{1}H-^{19}F couplings from crowded NMR spectra.[5] Subsequently, the obtained scalar couplings are converted to torsion angles using Karplus relations[6,7] which are then translated into five-membered ring pseudorotation angles (*P* and v_{max}) by means of the Altona-Sundaralingam formalism.[8] These two parameters completely describe the ring pucker. The results of the conformational analysis and impact of various fluorine substitution patterns will be presented in detail.

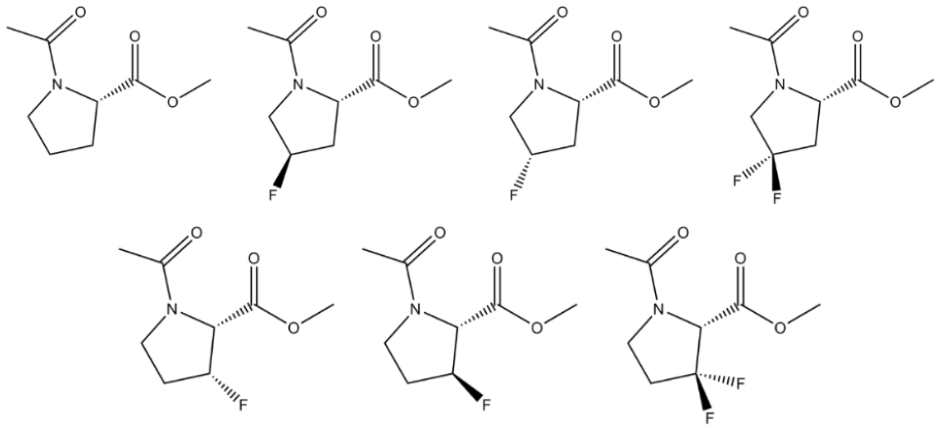

Figure 1. From top to bottom, left to right: Ac-Pro-OMe, Ac-(4*R*)-FPro-OMe, Ac-(4*S*)-FPro-OMe, Ac-4,4-F_2Pro-OMe, Ac-(3*R*)-FPro-OMe, Ac-(3*S*)-FPro-OMe and Ac-3,3-F_2Pro-OMe.

1. Kay, B.K, Williamson, M.P. and Sudol, M. *FASEB J.* 2000, **14**, 231.
2. Thomas, K.M., Naduthambi, D., Tririya, G. and Zondlo, N.J. *Org. Lett.*, 2005, **7**, 2397.
3. O'Hagan, D., *Chem. Soc. Rev.* 2008, **37**, 308.
4. Salwiczek, M., Nyakatura, E.K., Gerling, U.I., Ye, S. and Koksch, B. *Chem. Soc. Rev.*, 2012, **41**, 2135.
5. Sinnaeve, D., Foroozandeh, M., Nilsson, M. and Morris, G.A. *Angew. Chem. Int. Ed. Engl.*, 2016, **55**, 1090.
6. Diez, E., San-Fabian, J. and Guilleme, J. *Mol. Phys.* 1989, **68**, 49.
7. Thibaudeau, C., Plavec, J. and Chattopadhyaya J. *J. Org. Chem.* 1998, **63**, 4967.
8. Altona, C. and Sundaralingam, M. *J. Am. Chem. Soc.* 1972, **94**, 8205.

Using NMR metabolomics to unravel the pathways underlying the host-microbiota crosstalk in cancer cachexia

S.A. Pötgens, N.M. Delzenne and L.B. Bindels

Metabolism and Nutrition, Louvain Drug Research Institute, Université catholique de Louvain, Brussels.

Cachexia is a multifactorial syndrome which results from the interaction of several pathological processes. It mainly leads to muscle atrophy and fat mass loss and affects especially patients with cancer. Cachexia decreases tolerance and likelihood of response to cancer treatment. Currently, a clear understanding of this syndrome and a concrete therapeutic strategy is lacking. Previous data clearly established that, in a mouse model of leukemia and cachexia (BaF model), dietary modulation of the gut microbiota has the ability to impact the host in terms of cancer progression, inflammation and fat mass loss.[1,2]

In this context, this *PhD* research project aims to investigate new metabolic pathways to get a better understanding of host-microbiota interactions in cancer-associated cachexia. To achieve this goal, we will use next-generation sequencing and ^{1}H-NMR metabolomics to characterize both the microbial ecosystem through bacterial DNA analyses and metabolic profiling of caecal content and feces, and host metabolism through blood, liver and intestinal tissues analyses. The thesis will be structured in three interrelated axes.

The first step will consist in the implementation of ^{1}H-NMR metabolomics. Implementation will be performed using liver samples from the C26 model, as preliminary data obtained through traditional biochemistry analyses suggest a deep impact of the presence of the cancer cell on hepatic metabolism. The C26 model consists in a subcutaneous injection of colon carcinoma cells and is the most widely used mouse model of cancer cachexia.[3] In a second step, we will systematically apply ^{1}H-NMR to samples isolated from mice and humans affected by cancer and cachexia. Metabolic alterations in two cachectic mouse models (BaF and C26 models) will be documented, both on the host and microbial sides. In parallel, gut microbiota composition will be analysed using Illumina MiSeq of the 16S rRNA gene. Integration of these data through multivariate and network analyses will allow us to draw hypotheses regarding the gut microbiota-host interactions in case of cancer cachexia. To further validate our observations, we will analyze the metabolic profile of feces, urine and blood isolated from patients suffering from acute myeloid leukemia (AML), in relationship with their fecal microbiota composition. Samples will be provided by the MicroAML study. In a third step, we will apply this integrative physiology approach to mechanistic/interventional mouse studies involving for instance microbiota-targeting nutrients.

With this PhD project, we aim to get a deeper insight on the relationship between gut microbiota alterations and host metabolism in cancer cachexia. In addition, we expect to pinpoint biomarkers reflecting the beneficial effect of microbiota modulation on the host. These biomarkers could help to evaluate pre- and probiotics efficiency in future clinical trials through non-invasive blood and fecal content analyses.

1. Bindels, L.B. and Thissen, J.-P., *Clinical Nutrition Experimental* 2016, **6**, 74–82.
2. Bindels, L.B. *et al.The ISME Journal* 2016, **10(6)**, 1456–1470.
3. Talbert, E.E. *et al. Journal of Cachexia, Sarcopenia and Muscle* 2014, **5(4)**, 321–328.

Simple and direct method to quantify PEG molecules grafted on gold nanoparticles using ^{1}H NMR spectroscopy

M. Retout, H. Valkenier, and G. Bruylants

Engineering of Molecular Nanosystems, Université libre de Bruxelles.
50 Avenue F.D. Roosevelt, 1050 Bruxelles, Belgium.

Gold nanoparticles (GNPs) are of particular interest for biomedical diagnostics and therapeutic applications because of their remarkable optical properties, ease of surface functionalization and presumed biocompatibility. They are generally functionalized with polyethylenglycol molecules (PEGs) in order to ensure their stability under physiological conditions. It is of interest to have GNPs functionalized with mixtures of PEGs, in a controlled ratio, to ensure both their stability and the presence of post-functionalizable groups.

The quantification of the PEG proportions on the GNPs is difficult and is most often only based on indirect methods measuring the fraction of ungrafted PEGs. We report here a simple and direct method to quantify the different populations of PEGs grafted *via* thiols on GNPs. We observed that GNPs can be dissolved using iodine without leading to any PEG degradation, contrary to what is observed with more frequently used *aqua regia*. The freed PEGs can then be simply quantified using ^{1}H NMR.

Our results show that there is no direct relation between the proportion of grafted PEGs and their initial concentration in solution, which confirms that grafting *via* a thiol group is difficult to control. We are developing a novel grafting method using calix[4]arens as anchor molecules, and testing the method using our iodine based quantification protocol.

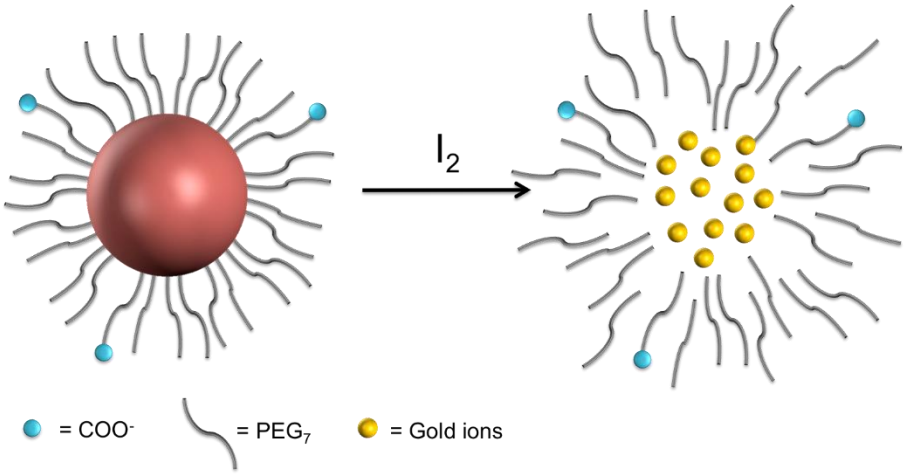

Figure 1: Dissolution with I_2 of a GNP functionalized with a mixture of two PEGs. After dissolution, PEG concentrations can be quantified by ^{1}H NMR.

Development of a sensitive and specific assay to measure mitochondrial superoxide in tumor cells

S. Scheinok[1], P. Levêque[1], P. Sonveaux[2] and B. Gallez[1].

[1] Biomedical Magnetic Resonance Research group, Louvain Drug Research Institute, UCL, Brussels.
[2] Pole of Pharmacology (FATH), Institut de Recherche Expérimentale et Clinique (IREC), UCL, Brussels.

Introduction: It has been recently suggested that mitochondrial superoxide production could promote cell migration, invasion and metastasis of cancer in mice.[1] MitoTempo, a superoxide scavenger, blocked this aggressiveness of cancer cells.[1] However, as it was reported that MitoTempo is not specific of the superoxide,[2] it would be desirable to validate a technique that could detect unambiguously the production level of mitochondrial superoxide in cancer cells. Nowadays there are three main techniques to detect superoxide anion: the use fluorescent probes, the electrochemical methods and the EPR-based techniques. We are focusing on the latter approach.

Aims : The overall aim of the thesis is to identify the most sensitive and specific approach to detect superoxide anion and to validate its use in mitochondria and cancer cells. This first year of research was focused on a systematic comparison of performances of new tools and their benchmarking with existing ones.

Methods: Two different approaches were evaluated. The first one is based on spin trapping (monitoring of the formation of a stable spin adduct (EPR detectable) after reaction with superoxide. We evaluate the spin trap capacity of 3 new compounds synthesized in our laboratory that were supposed to give stable trityl radical after reaction with superoxide. We also used the classical nitrone spin traps (EMPO, DEPMPO, DIPPMPO). The second approach was based on the decay of stable free radicals in the presence of superoxide. Compounds tested included nitroxides (Tempol, mitoTempo) and trityl radicals (CT-03 and PCT) in the presence of superoxide anion. The experiments were performed in vitro at 310K. The superoxide radical was produced using a hypoxanthine (1mM)/xanthine oxidase system. Five concentrations of xanthine oxidase (0,05; 0,02; 0,01; 0,005; 0,0017 U/ml) were used to compare the sensitivity of the different probes. Hydroxyl radical was also produced with a Fenton reaction (H_2O_2:1mM) to test the specificity of the probes towards the superoxide radical.

Results: a) Spin trapping: The new class of synthesized compounds provide an EPR signal after reaction with superoxide. However, the analysis of the EPR signal revealed that the radical obtained was not a direct spin adduct due to the reaction with superoxide but due to further molecules rearrangements. This makes these compounds non useful for our purpose. In contrast, nitrone spin traps detected superoxide even when the enzyme concentration was low. The relative sensitivity for the detection of superoxide was DIPPMPO>EMPO>DEPMPO.
b) Decay of EPR signal: The EPR signal of nitroxides (Tempol, mitoTempo) and of trityl radicals (CT-03 and PCT) decreased rapidly in the presence of superoxide while hydroxyl radical had negligible effect. The highest sensitivity was observed for the trityl radicals.

Conclusions and short-term perspectives: We are now testing the performance of the best candidates (DIPPMPO for spin trapping) and trityls (for the decay approach) in tumor cells and mitochondria isolated from tumor cells.

1. Porporato, P. E., Payen, V. L., Pérez-Escuredo, J., De Saedeleer, C. J., Danhier, P., Copetti, T., Dhup, S., Tardy, M., Vazeille, T., Bouzin, C., Feron, O., Michiels, C., Gallez, B. and Sonveaux, P. *Cell Reports* 2014, **8**: 754–766.
2. Samuni, A., Goldstein, S., Russo, A., Mitchell, J. B., Krishna, M. C. and Neta. P. J. Am. Chem. Soc. 2002, **124**, No. 29: 8719-8724.

Palladium-based chemosensors for the characterization of raw plant extracts by ^{19}F NMR spectroscopy

F. Souard[1], V. Piras[1,2], R. D'Orazio[3], L. Stefanosaka[3], F. Dufrasne[4], P. Stoffelen[5], C. Stévigny[1] and M. Luhmer[2,3]*

[1] *Laboratoire de Pharmacognosie, Bromatologie et Nutrition humaine (PlantNut) – ULB CP 205/09.*
[2] *Laboratoire de Résonance Magnétique Nucléaire Haute Résolution (RMN-HR) – ULB CP 160/08.*
[3] *Centre d'Instrumentation en REsonance Magnétique (CIREM) – ULB CP 160/08.*
[4] *Chimie Pharmaceutique Organique (CPO) – ULB CP 205/05.*
[1-4] *Université libre de Bruxelles (ULB),* [5]*Jardin Botanique de Meise.*
* *to whom correspondence should be addressed: michel.luhmer@ulb.ac.be*

Detection of natural biogenic compounds is of utmost importance in many fields and methods that operate in complex mixtures without the need for pretreatment and/or separation techniques are obviously highly desirable. According to a recent work of Zhao *et al.*, fluorinated pincer-type palladium(II) complexes are promising chemosensors for the detection of amines and N-heterocycles by ^{19}F NMR.[1] The palladium complexes studied so far exhibit two identical aromatic subunits decorated with equivalent fluorine atoms or fluorinated groups. They give rise to a unique ^{19}F NMR signal and discrimination between analytes therefore relies on a one-dimensional chemical shift map.

With the purpose of increasing the discrimination power using a two-dimensional ^{19}F chemical shift map, while maintaining similar detection limits, analog palladium complexes comprising aromatic groups bearing non-equivalent fluorine probes were designed (Figure 1) and such a first chemosensor was synthesized.

NMR experiments carried out for the validation of the method will be described and preliminary results of its application for the characterization of raw plant extracts will be presented.

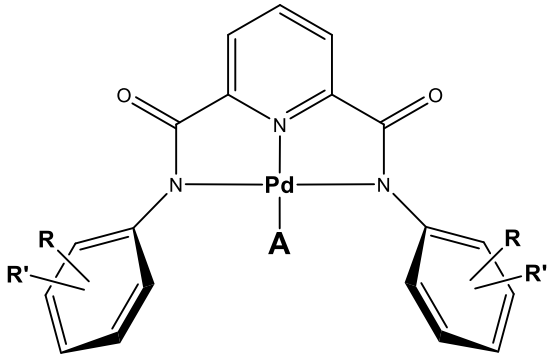

Figure 1: Generic structure of the pincer-type palladium(II) chemosensor designed for the discrimination of analytes in complex mixtures using a two-dimensional ^{19}F chemical shift map. **R** and **R'** are non-equivalent fluorine-containing groups, **A** stands for analyte (amine or N-heterocyclic compound, notably).

1. Zhao Y., Chen L., Swager T.M. *Angew. Chem. Int. Ed.* 2016, **55**, 917-921.

^{31}P solid state NMR for the quantitative characterization of TiO_2 nanopowders modified with phosphonic acids

M. Tassi, G. Reekmans, J. D'Haen, R. Carleer and P. Adriaensens

Applied and Analytical Chemistry, Institute for Materials Research (IMO), Hasselt University, Agoralaan 1 - Building D, B-3590 Diepenbeek.

The reaction mechanism of the reaction between titanium dioxide (P25 TiO_2) nanopowder and phenyl phosphonic acid (PPA) is explored thoroughly and the influence of the reaction conditions on the formed products is presented. This modification can result in grafting of the phosphonic acid at the nanocrystal surface as well as in the formation of titaniumphenylphosphonate lamellar structures. The formation of titaniumphenylphosphonate is favored at increasing reaction temperatures[1]. Calcination experiments (at 600 and 1000 °C) elucidated that the presence of amorphous TiO_2[2] is a crucial factor in the formation of titaniumphosphonate. It was established that in water and at temperatures above 45°C, the dissolution of amorphous TiO_2 leads to the formation of these lamellar structures. This in contrast to the grafting of phosphonic acids at the TiO_2 surface which is independen of the reaction temperature. The grafting mechanism involves the protonation of the surface hydroxyl groups, followed by the nucleophilic attack of the phosphonic acid and simultaneous release of water. The formation of covalent bonds between titanium and the phosphonic group (P-O-Ti bonds) and the amounts of surface grafting and titaniumphosphonate formation are quantitatively determined, using an internal standard, with ^{31}P MAS SS-NMR[3,4]. The broad signal situated at between 0-20 ppm results from the phosphonic acid grafting, while the signal around -8 ppm originates from titaniumphosphonate. TEM images and spin-diffusion path lengths indicate titaniumphosphonate crystal dimensions between 25 and 550 nm depending on the reaction conditions. The results indicate that the amount of PPA involved in titaniumphenylphosphonate crystals increases for higher reaction temperatures while the amount of phosphonic acid grafting remains constant.

1. Mutin, P. H., Guerrero, G., Vioux, A. *J. Mater. Chem.* 2005, **15**, 3761–3768.
2. Ohno, T., Sarukawa, K., Tokieda, K., Matsumura, M. *J. Catal.* 2001, **203**, 82–86.
3. Guerrero, G., Mutin, P. H., Vioux, A. *Chem. Mater.* 2001, **13**, 4367–4373.
4. Souma, H., Chiba, R., Hayashi, S. *Bull. Chem. Soc. Jpn.* 2011, **84**, 1267–1275.
5. Hosseinabadi, R. S., Wyns, K., Meynen, V., Carleer, R., Adriaensens, P., Buekenhoudt, A., Van der Bruggen, B. *J. Membrane Science* 2014, **454**, 496–504.

Synthesis and characterization of a nanoparticulate T1 contrast agent for magnetic resonance imaging

T. Vangijzegem[1], D. Stanicki[1], S. Boutry[2], R.N. Muller[1,2], L. Vander Elst[1,2] and S. Laurent[1,2]

[1] Department of General, Organic and Biomedical Chemistry, NMR and Molecular Imaging Laboratory, University of Mons, 7000 Mons, Belgium.
[2] CMMI – Center for Microscopy and Molecular Imaging, 6041 Gosselies, Belgium.

The design of novel contrast agents exhibiting enhanced effectiveness is a real concern in the field of magnetic resonance imaging (MRI). Indeed, contrast agents are often needed to overcome the poor sensitivity of the technique. Among these agents, iron oxide nanoparticles are of great interest thanks to their remarkable magnetic properties. However, the negative contrast induced by such species has limited their use in clinical goals. Interestingly, it was recently showed that small-sized (< 5 nm) iron oxide nanoparticles are able to generate T_1 enhanced images[1,2].

This work reports the development and the characterization of iron oxide nanoparticles with a small iron oxide core and a stabilizing coating. Such systems could act as new T_1 contrast agents for MRI.

In the present work, iron oxide nanoparticles were obtained by a thermal decomposition method (magnetic core size of 4,2 ± 0,4 nm). The contrast agent was then obtained by mean of a ligand exchange protocol with a PEG-based ligand anchored onto the nanoparticles surface through a biphosphonate moiety.

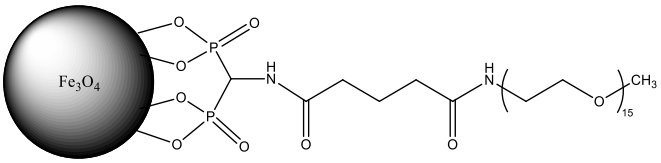

Scheme of the contrast agent

The potential of our platform as a T_1 contrast agent has been demonstrated through characterization of its relaxometric properties. Indeed, these nanoparticles are characterized by a high longitudinal relaxivity value (at 20 and 60 MHz) along with a small r_2/r_1 ratio. Moreover, our system has been tested in a first *in vivo* experiment performed at the Center for Microscopy and Molecular Imaging (CMMI). MRI pictures obtained show a significant contrast enhancement in the vena cava, confirming the potential of our system for MRI and more specifically for an application in MRI angiography.

1. Kim, B. H. *et al*. *J. Am. Chem. Soc.* 2011, **133,** 12624–12631.
2. Taboada, E. *et al*. *Langmuir* 2007, **23,** 4583–4588.

EPR study of lead-free $MA_2CuCl_xBr_{4-x}$ hybrid perovskites for photovoltaics

M. Van Landeghem[1], E. Goovaerts[1] and S. Van Doorslaer[2]

[1] *Experimental Condensed Matter Physics, Department of Physics, University of Antwerp.*
[2] *BIMEF Laboratory, Department of Physics, University of Antwerp.*

Over the last 6 years the power conversion efficiency of lead-halide perovskite solar cells has skyrocketed from an initial value of 4% to over 20% today. This result is even more impressive considering the exceptionally relaxed processing requirements of perovskite solar cells enabling room-temperature solution processing techniques. However, the pollution risk and toxicity related to the high Pb-content of the perovskite absorber layer raises concerns about the viability of future commercial applications. Hence current research interest focuses on replacing the Pb^{2+} by earth abundant and environmentally friendly transition metals such as Fe^{2+}, Cu^{2+} or Zn^{2+} while preserving the excellent photovoltaic performance.

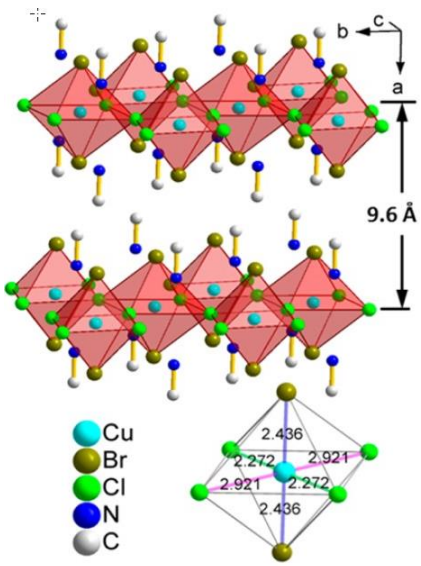

In this context we investigated a series of Cu-based hybrid perovskites $MA_2CuCl_xBr_{4-x}$ which were recently identified as an interesting paradigm in the search for lead-free alternatives.[1] The crystal structure of the two-dimensional perovskite $MA_2CuCl_2Br_2$ is depicted in the figure (taken from [1]) showing the alternating organic and inorganic layers. The main motivation for choosing divalent Cu^{2+} as a replacement for Pb^{2+} arose from the high stability of this oxidation state in ambient air and its ability to form compounds with large absorption coefficient in the visible region. However, the high density of unpaired electrons due to the Cu^{2+} ions in $MA_2CuCl_xBr_{4-x}$ seems to hamper electronic transport, in particular hole transport, as illustrated by the poor power conversion efficiencies of 0.017% in devices using $MA_2CuCl_2Br_2$ as a sensitizer.[1]

Here we present an EPR study of $MA_2CuCl_2Br_2$ and MA_2CuCl_4 crystallites in order to gain a better understanding of the bulk material properties of Cu perovskites. We studied light-induced formation of Cu^+ trap states as reported by D. Cortecchia et al.[1] yet no effect was observed in the EPR spectrum. Moreover, building on earlier studies on 2D Cu perovskites regarding their intriguing magnetic properties,[2-4] we investigated the (anti-) ferromagnetic phase transition at low temperatures (~10K) mediated by the superexchange interaction between Cu-centers via adjacent halide bonds.

1. Cortecchia, D. et al. *Inorg. Chem.* 2016, **55**, 1044-1052.
2. Zolfaghari, P., de Wijs, G. A., de Groot, R. A. *J. Phys.: Condens. Matter* 2013, **25**, 295502.
3. Lee, C. H., Lee, K. W., Lee, C. E. *Current Applied Physics* 2003, 447-479.
4. Fedoseeva, N. V., Volkov, N. V., Patrin, G. S. *Physics of the Solid State* 2003, **45**, 499-502.

Porous Sn-silicate catalysts prepared *via* aerosol-assisted sol-gel process

A. Vivian[1], L. Fusaro[1], D. P. Debecker[2] and C. Aprile[1]

[1] *Unit of Nanomaterial Chemistry (CNano), Department of Chemistry, University of Namur*
[2] *Institute of Condensed Matter and Nanoscience - Molecules, Solids and Reactivity (IMCN/MOST), Université catholique de Louvain.*

Recently, growing efforts are being devoted to transform glycerol and its derivatives into valuable chemicals employing various catalytic processes.[1] One of the most attractive synthesis procedures is represented by the synthesis of ethyl lactate from dihydroxyacetone, which can itself be easily obtained by partial oxidation of glycerol. In order to achieve high yield of ethyl lactate a catalyst displaying a combination of Lewis and mild Brønsted acid sites is required. Sn-doped silica catalysts, possessing the good combination of acid sites, have already been reported as active and versatile catalysts for the conversion of dihydroxyacetone into ethyl lactate.[2] Moreover, it was observed that the reduced particle size together with the good dispersion of Sn inserted as single site in the silica architecture are key factors to improve the activity of the catalyst.

Here we prove that the aerosol-assisted sol-gel process[3] offers a unique opportunity for the preparation of active and efficient Sn-silicate catalysts. The advantages of this process compared to conventional sol-gel approaches include: a limited number of steps, a continuous production and collection of the material and a limited production of wastes, making this process also interesting from a sustainable point of view.[4]

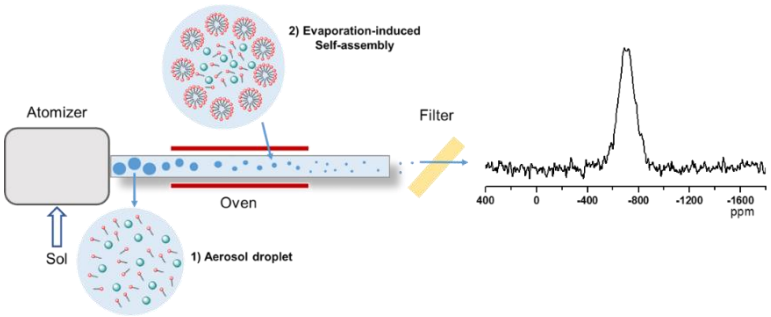

Figure 1: Schematic representation of the aerosol-assisted self-assembly process and example of ^{119}Sn static NMR spectrum of the synthesized solids

A series of Sn-silicate nanoparticles were synthesized taking inspiration from a previously reported method.[3] The solids were extensively characterized *via* N_2 physisorption, XRD, TEM, ICP-OES, EDX and DR-UV-vis. Moreover, a deeper structural investigation of the materials was performed *via* solid-state ^{29}Si-MAS NMR and ^{119}Sn static NMR. ^{29}Si cross-polarization and direct-excitation quantitative experiments were used to obtain insights about the environment of the different ^{29}Si contributions and evaluate the degree of condensation of the materials. ^{119}Sn-NMR showed unambiguously that Sn was predominantly inserted in tetrahedral coordination. Octahedrally coordinated extra-framework SnO_2 was not observed. The observed signal, centered at around –695 ppm, was attributed to intra-framework Sn(IV) and was not affected by the hydration degree. These aerosol-made Sn-silicates showed excellent catalytic performance in the conversion of dihydroxyacetone to ethyl lactate both in terms of yield and selectivity.

1. Pagliaro, M., Ciriminna, R., Kimura, H., Rossi M. and Della Pina C. *Angew. Chem. Int. Ed.* 2007, **46**, 4434-40
2. Li, L., Collard, X., Bertrand, A., Sels, B. F., Pescarmona P. P., and Aprile, C. *J. Catal.* 2014, **314**, 56-65
3. Debecker, D. P., Stoyanova, M., Rodemerck, U., Colbeau-Justin, F., Boissère, C., Chaumonnot, A., and Sanchez, C. *Appl. Catal. A* 2014, **470**, 458-466.
4. Boissière, C., Grosso, D., Chaumonnot, A. Nicole, L. and Sanchez, C. *Adv. Mater*. 2011, **23**, 599-623

LIST OF PARTICIPANTS

Last Name	First name	Affiliation	E-Mail
Acciardo	Stefania	UCL	stefania.acciardo@uclouvain.be
Adriaensens	Peter	UHasselt	peter.adriaensens@uhasselt.be
Aprile	Carmela	UNamur	carmela.aprile@unamur.be
Atzori	Luciano	UNamur	lucianoatzori@hotmail.it
Barakat	Tarek	UNamur	tarek.barakat@unamur.be
Bartik	Kristin	ULB	kbartik@ulb.ac.be
Bindels	Laure	UCL	laure.bindels@uclouvain.be
Bivona	Lucia Anna	UNamur	lucia.bivona@unamur.be
Brindle	Kevin	University of Cambridge	kmb1001@cam.ac.uk
Bruylants	Gilles	ULB	gbruylan@ulb.ac.be
Capette	Loïc	UMONS	loic.capette@umons.ac.be
Carbonell	Esther	UNamur	esther.carbonell@unamur.be
Chilla	Satya	Umons	Satya.chilla@umons.ac.be
Cinà	Valerio	UNamur	valerio.cina.vc@gmail.com
Comès	Adrien	UNamur	adrien.comes@unamur.be
Damblon	Christian	ULg	c.damblon@ulg.ac.be
Dandois	Yannick	UGent	yannick.dandois@ugent.be
Danhier	Pierre	UCL	pierre.danhier@uclouvain.be
Delevoye	Laurent	Université de Lille	laurent.delevoye@ensc-lille.fr
Delneuville	Cyrille	UNamur	cyrille.delneuville@unamur.be
Denis	William	ULB	wdenis@ulb.ac.be
Desmet	Céline	UCL	celine.m.desmet@uclouvain.be
de Tullio	Pascal	ULg	p.detullio@ulg.ac.be
Diricq	Jérôme	UMONS	jerome.diricq@umons.ac.be
Emilio	Brunetti	ULB	ebrunett@ulb.ac.be
Fehér	Krisztina	UGent	krisztina.feher@ugent.be
Florian	Gourgue	UCL	florian.gourgue@uclouvain.be
Fusaro	Luca	UNamur	luca.fusaro@unamur.be
Gallez	Bernard	UCL	bernard.gallez@uclouvain.be

Geudens	Niels	UGent	niels.geudens@ugent.be
Gossuin	Yves	Umons	Yves.gossuin@umons.ac.be
Govaerts	Kristof	KU Leuven	kristof.govaerts@med.kuleuven.be
Grauwels	Glenn	ULB	glenn.grauwels@ulb.ac.be
Hafideddine	Zainab	UAntwerpen	Zainab.Hafideddine@uantwerpen.be
Hannecart	Adeline	UMONS	adeline.hannecart@umons.ac.be
Henoumont	Céline	UMONS	celine.henoumont@umons.ac.be
Henrard	Daniel	UMONS	daniel.henrard@umons.ac.be
Hequet	Emilie	UMONS	Emilie.HEQUET@student.umons.ac.be
Himmelreich	Uwe	KU Leuven	uwe.himmelreich@kuleuven.be
Jordan	Benedicte	UCL	benedicte.jordan@uclouvain.be
Kay	Jennifer	ULg	j.kay@doct.ulg.ac.be
Kilani	Farah	UNamur	kilanifarah@hotmail.fr
Kovacs	Benjamin	UMONS	Benjamin.Kovacs@UGent.be
Kozlova	Arina	UCL	arina.kozlova@uclouvain.be
Laurent	Sophie	UMONS	sophie.laurent@umons.Ac.be
Leenders	Justine	ULg	jleenders@ulg.ac.be
le Paige	Ulric	Leiden Universiteit	u.b.a.le.paige@lic.leidenuniv.nl
Leveque	Philippe	UCL	philippe.leveque@uclouvain.be
Licini	Giulia	University of Padova, IT	giulia.licini@ulb.ac.be
Luhmer	Michel	ULB	michel.luhmer@ulb.ac.Be
Luong	Thi Kim Nga	KU Leuven	thikimnga.luong@kuleuven.be
Ly Thi	Hong Giang	KU Leuven	honggiang.lythi@kuleuven.be
Marcelis	Lionel	UCL	lionel.marcelis@uclouvain.be
Martins	Jose	UGent	Jose.Martins@UGent.be
Michez	Roman	ULB	rmichez@ulb.ac.be
Mignion	Lionel	UCL	lionel.mignion@uclouvain.be
Montante	Sylvie	UMONS	sylvie.montante@umons.ac.be
Muller	Robert	UMONS	ROBERT.muller@umons.ac.be
Neveu	Marie-Aline	UCL	marie-aline.neveu@uclouvain.be
Nys	Kevin	UAntwerpen	kevin.nys@uantwerpen.be
Ottoy	Emile	UGent	emile.ottoy@ugent.be
Piras	Veronica	ULB	pirasvnc@gmail.com

Potgens	Sarah	UCL	sarah.potgens@uclouvain.be
Reekmans	Gunter	UHasselt	gunter.reekmans@uhasselt.be
Reiter	Nicolas	UMONS	nicolas.reiter@student.umons.ac.be
Retout	Maurice	ULB	mretout@ulb.ac.be
Scheinok	Samantha	UCL	samantha.scheinok@uclouvain.be
Schoonjans	Céline	UCL	celineschoonjans@gmail.com
Schoumacher	Matthieu	ULg	m.schoumacher@ulg.ac.be
Silvanose	Biju	KU Leuven	biju.silvanose@kuleuven.be
Sinnaeve	Davy	UGent	Davy.Sinnaeve@UGent.be
Souard	Florence	ULB - Université Grenoble Alpes	florence.souard@univ-grenoble-alpes.fr
Spillier	Quentin	UCL	quentin.spillier@uclouvain.be
Sudakov	Ivan	UAntwerpen	Ivan.Sudakov@uantwerpen.be
Thabault	Leopold	UCL	Leopold.thabault@uclouvain.be
Tumanov	Nikolay	UNamur	nikolay.tumanov@unamur.be
Valkenier	Hennie	ULB	hennie.valkenier@ulb.ac.be
Van Doorslaer	Sabine	UAntwerpen	sabine.vandoorslaer@uantwerpen.be
Van Landeghem	Melissa	UAntwerpen	melissa.vanlandeghem@uantwerpen.be
Vander Steen	Julien	ULB	jvdsteen@ulb.ac.be
Vangijzegem	Thomas	UMONS	thomas.vangijzegem@student.umons.ac.be
Vivian	Alvise	UNamur	alvise.vivian@unamur.be
Volkov	Alex	VIB-VUB	ovolkov@vub.ac.be
Vuong	Quoc Lam	UMONS	quoclam.vuong@umons.ac.be
Wanko	Marius	ULg	amwanko@doct.ulg.ac.be
Vivian	Alvise	UNamur	alvise.vivian@unamur.be

The organizing committee gratefully acknowledges the following institutions, societies and companies for their kind support

Platinum Sponsors

Golden Sponsors

Silver Sponsors